The Gannon Storm: citizen science observations during the geomagnetic superstorm of 10 May 2024

Maxime Grandin[1,2]**, Emma Bruus**[3,4]**, Vincent E. Ledvina**[5,6]**, Noora Partamies**[7]**, Mathieu Barthelemy**[8,9]**,
Carlos Martinis**[10]**, Rowan Dayton-Oxland**[11]**, Bea Gallardo-Lacourt**[12,13]**, Yukitoshi Nishimura**[14]**, Katie Herlingshaw**[7]**,
Neethal Thomas**[3]**, Eero Karvinen**[4]**, Donna Lach**[6,15]**, Marjan Spijkers**[16]**, and Calle Bergstrand**[17]

[1]Department of Physics, University of Helsinki, Helsinki, Finland
[2]Finnish Meteorological Institute, Helsinki, Finland
[3]Sodankylä Geophysical Observatory, University of Oulu, Sodankylä, Finland
[4]Taivaanvahti/Skywarden Observation Service, Ursa Astronomical Association, Helsinki, Finland
[5]Geophysical Institute, University of Alaska Fairbanks, Fairbanks, AK, USA
[6]Aurorasaurus, New Mexico Consortium, Los Alamos, NM, USA
[7]Department of Arctic Geophysics, University Centre in Svalbard, Longyearbyen, Norway
[8]IPAG, Université Grenoble Alpes, CNRS, Grenoble, France
[9]CSUG, Université Grenoble Alpes, Grenoble, France
[10]Physics and Astronomy, Center for Space Physics, Astronomy Department, Boston University, Boston, MA, USA
[11]University of Southampton, Southampton, United Kingdom
[12]Goddard Space Flight Center, National Aeronautics and Space Administration, Greenbelt, MD, USA
[13]Department of Physics, The Catholic University of America, Washington, DC, USA
[14]Department of Electrical and Computer Engineering and Center for Space Physics, Boston University, Boston, MA, USA
[15]citizen scientist, Canada
[16]citizen scientist, the Netherlands
[17]citizen scientist, Sweden

Correspondence: Maxime Grandin (maxime.grandin@fmi.fi)

Abstract. The 10 May 2024 geomagnetic storm, referred to as the Gannon Storm in this paper, was one of the most extreme to have occurred in over 20 years. In the era of smartphones and social media, millions of people from all around the world were alerted to the possibility of exceptional auroral displays. Hence, many people not only witnessed but also photographed the aurora during this event. These citizen science observations, although not from scientific instruments operated by observatories or research groups, can prove to be invaluable in obtaining data to characterise this extraordinary event. In particular, many observers saw and photographed the aurora at mid-latitudes, where ground-based instruments targeting auroral studies are sparse or absent. Moreover, the proximity of the event to the Northern Hemisphere summer solstice meant that many optical instruments were not in operation due to the lack of suitably dark conditions. We created an online survey and circulated it within networks of aurora photographers to collect observations of the aurora and of disruptions in technological systems that were experienced during this superstorm. We obtained 696 citizen science reports from over 30 countries, containing information such as the time and location of aurora sightings and the observed colours and auroral forms, as well as geolocalisation, network, and power disruptions noticed during the geomagnetic storm. We supplemented the obtained dataset with 186 auroral observations logged in the Skywarden catalogue (https://taivaanvahti.fi, last access: 19 December 2024) by citizen scientists. The main findings enabled by the data collected through these reports are that the aurora was widely seen from locations at geomagnetic latitudes

ranging between 30 and 60°, with a few reports from even lower latitudes. This was significantly further equatorward than predicted by auroral oval models. The reported auroral emission colours, predominantly red and pink and intense enough to reach naked-eye visibility, suggest that the auroral electron precipitation contained large fluxes of low-energy ($<$ 1 keV) particles. This study also reveals the limitations of citizen science data collection via a rudimentary online form. We discuss possible solutions to enable more detailed and quantitative studies of extreme geomagnetic events with citizen science in the future.

---

1 Introduction

The aurora has captivated human beings since ancient times, with some of the earliest reports being found in an ancient Chinese annal known as the Bamboo Annals and mentioning auroral observations from near Xi'an dating from either 977 ± 1 BCE or 957 ± 1 BCE (Usoskin et al., 2023). Typically visible at high latitudes around Earth's poles, the aurora can be seen further equatorward during geomagnetic storms (e.g. Blake et al., 2021). Such was the case during the extreme geomagnetic storm starting on 10 May 2024, which was the most intense geomagnetic storm since the so-called Halloween storms of October–November 2003 over 20 years ago (Greshko, 2024). Two names have been put forward to refer to the 10 May 2024 superstorm: the "Mother's Day Storm" (as it occurred over Mother's Day weekend in some countries) or the "Gannon Storm" (in memory of Dr. Jennifer Gannon). In this paper, we will retain the name of "Gannon Storm", both to honour Dr. Gannon's memory and to acknowledge the fact that Mother's Day does not have a universal date across countries. The multiple coronal mass ejections (CMEs) from the Sun, which led to this geomagnetic storm, originated from a large and complex cluster of sunspots 16 times the diameter of Earth (Spogli et al., 2024; Kwak et al., 2024). The plasma parameters and interplanetary magnetic field associated with these interacting CMEs produced exceptional driving conditions when encountering the Earth's magnetosphere.

The consequences of extreme geomagnetic storms are not negligible. Human-made space-borne and ground-based infrastructure can be significantly affected. Hapgood et al. (2021) give an interesting overview of the potential space weather effects of such extreme events, focusing on British infrastructure. These include threats to power grid systems posed by geomagnetically induced currents, impacts on satellite communication and global navigation satellite systems (GNSSs), blackouts and anomalous propagation of high-frequency radio signals, damage to the onboard electronics of satellites, increased atmospheric drag for low-Earth-orbiting satellites, and effects on civil aviation due to enhanced radiation doses in the polar regions. A few studies

have undertaken estimations of the potential financial cost of space weather impacts and found values ranging from millions to tens of billions of US dollars per day, corresponding to 15 %–100 % of the daily US GDP, depending on the tested scenario (Oughton et al., 2017), or a total of up to a few trillion US dollars in the case of a Carrington-level superstorm (Eastwood et al., 2018). The September 1859 "Carrington" event is one of the largest storms ever documented for which geomagnetic indices have been estimated (Siscoe et al., 2006). Much more recently, the 23 July 2012 extreme coronal mass ejection (CME) which was not Earth-directed could have produced a geomagnetic storm on par with – if not more intense than – the Carrington Storm (Baker et al., 2013). The aforementioned studies of the financial costs of space weather further underline that the obtained estimates bear large uncertainties as evaluating the total costs for economy increasingly relying on technology is extremely challenging.

When extreme geomagnetic storms occur, the auroral ovals extend equatorward, usually beyond the regions where most of the ground-based scientific instruments (optical and radar) designed for space physics studies are located (e.g. Johnsen, 2013; Kataoka et al., 2024). Therefore, the most severe events are likely not to be properly captured by our routine science observations apart from the few instruments at mid-latitudes and satellite measurements which inherently provide sparse coverage. For instance, the Super Dual Auroral Radar Network (SuperDARN; Nishitani et al., 2019) mid-latitude radars provide an uneven coverage across longitudes, with large gaps in the European, Russian, and southern mid-latitude sectors. Superstorms are also poorly described by numerical models as the driving conditions lie beyond the regime of their validity. For instance, the OVATION Prime model of the auroral oval (Newell et al., 2014) has been fitted for driving conditions up to those corresponding to Kp index values of 8+. During the Gannon Storm, the Kp index reached the value of 9 during three 3 h periods (Spogli et al., 2024). As extreme conditions are largely absent from training datasets, AI-based models are currently limited in making realistic forecasts of geomagnetic conditions during superstorms (e.g. Oliveira et al., 2021).

For these reasons, finding other data sources to study the most extreme geomagnetic storms such as the Gannon Storm is necessary. With the recent tremendous improvement in commercially available off-the-shelf (COTS) and smartphone camera systems, large numbers of people now have the capability to take relatively high-quality photos of the aurora and night sky. Using such images as data for scientific studies has proved successful in a growing number of studies which showcase examples of citizen science applied to space physics. Often, those studies have made use of selected photographs of the aurora taken by citizen scientists to investigate elusive optical phenomena for which observations by scientific instruments were either missing or not sufficient. For instance, the phenomenon known as STEVE

(a backronym for strong thermal emission velocity enhancement) was first uncovered thanks to citizen scientists (MacDonald et al., 2018) and is often accompanied by vertical green structures dubbed as the picket fence. STEVE and the picket fence have given rise to numerous publications relying on citizen science imagery (e.g. Archer et al., 2019; Mende and Turner, 2019; Martinis et al., 2021; Nishimura et al., 2023). Furthermore, the relationship between STEVE and stable auroral red (SAR) arcs has been examined thanks to citizen science (Martinis et al., 2022). Emission structures of very small spatial scales have also been investigated involving citizen scientists, either using photographs they took (e.g. the so-called "streaks" occasionally seen along with the picket fence; Semeter et al., 2020) or having them participate in auroral-form classification (e.g. fragmented aurora-like emissions; Whiter et al., 2021). Finally, "dunes", which exhibit wave-like patterns in the diffuse green aurora, have also been investigated largely relying on citizen science data from auroral photographers (Palmroth et al., 2020; Grandin et al., 2021; He et al., 2023).

Citizen science applied to space physics has the potential to produce scientifically valuable data not only for the study of specific phenomena, as discussed above, but also by providing an agile way to collect observations on a more general level (Ledvina et al., 2023). Collaborative aurora-sighting reporting platforms such as Aurorasaurus (MacDonald et al., 2015) have proved to be very powerful in providing ground-truth validation of auroral boundaries derived from empirical models (Kosar et al., 2018b). Aurorasaurus has also demonstrated its efficacy in generating auroral visibility alerts in real time (Case et al., 2016a). Moreover, the submitted auroral visibility reports can be accompanied by images which are geotagged and made available for scientific use after validation (Kosar et al., 2018a). Another collaborative catalogue of observations providing invaluable data for auroral studies is Skywarden (https://taivaanvahti.fi, last access: 19 December 2024; from its original Finnish name: Taivaanvahti; see Sect. 3). This aurora observation platform, established in 2011 (Karttunen, 2021), contains more than 10 000 open-access, content-verified auroral observations accompanied by one or several photographs. Skywarden's observations have been used in relation to the dunes (Palmroth et al., 2020), in the discovery of proton-injection-initiated red arcs with green diffuse aurora (Nishimura et al., 2022), and in research of other atmospheric and astronomical phenomena (Gritsevich et al., 2014; Moilanen and Gritsevich, 2022).

The Gannon Storm was the first geomagnetic event of such magnitude occurring during the era of social media and COTS cameras and smartphones capable of photographing the aurora. Therefore, it is an unprecedented opportunity to investigate to what extent citizen scientists can provide observations that could be used to improve our characterisation of processes occurring during extreme geomagnetic storms. It is also a unique opportunity to estimate how many citizen scientists from all around the world can be mobilised to provide reports on what they saw during the event, including those who had no prior experience with auroral observations and were not aware of projects like Skywarden or Aurorasaurus. To test these ideas, the ARCTICS (Auroral Research Coordination: Towards Internationalised Citizen Science, https://collab.issibern.ch/arctics/, last access: 19 December 2024) working group supported by the International Space Science Institute in Bern, Switzerland, conducted an online survey which was distributed as widely as possible among our network of collaborators and among online networks of aurora chasers. This survey enabled citizen scientists to report whether they saw the aurora or experienced disruptions in technological systems during the superstorm (see Sect. 3).

The objective of this paper is to evaluate how much data can be collected thanks to citizen science during extreme geomagnetic events and what kind of scientifically usable information can be obtained from citizen scientist observations. We will pay particular attention to scientific results that would prove to be difficult to obtain relying solely on existing scientific instruments and models. Section 2 presents the geophysical context of the Gannon Storm. Section 3 describes the collection and pre-processing of citizen science observations of the aurora and technological disruptions during the storm, and in Sect. 4, we analyse the citizen science data and examine what scientific conclusions regarding the storm can be inferred from this dataset. We discuss the limitations and challenges of the collected citizen science observations and propose solutions to overcome them in Sect. 5, and we summarise our findings in Sect. 6.

2 Geophysical context

Between 8 and 10 May 2024, an Earth-facing sunspot region, AR 3664, produced multiple X-class flares associated with halo CMEs, indicating their propagation towards the Earth. These CMEs may have collided and merged, resulting in a complex magnetic cloud structure. When this CME structure reached the Earth, it triggered a geomagnetic storm categorised as "extreme" (G5 class according to the NOAA Space Weather Scales, https://www.swpc.noaa.gov/noaa-scales-explanation, last access: 19 December 2024). A detailed analysis of the driving conditions and of the global geomagnetic response they led to can be found in Kwak et al. (2024).

We retrieved the provisional 1 h OMNI data (Papitashvili and King, 2020) to visualise the key interplanetary magnetic field (IMF) and solar wind parameters during 10–13 May 2024. Those data have been measured by various spacecraft orbiting around the L1 Lagrange point of the Sun–Earth system and propagated to the terrestrial bow shock. Figure 1 shows the time series of the solar wind and IMF parameters during the event. The IMF magnitude (black line) and B_z (north–south) component (red line) are presented
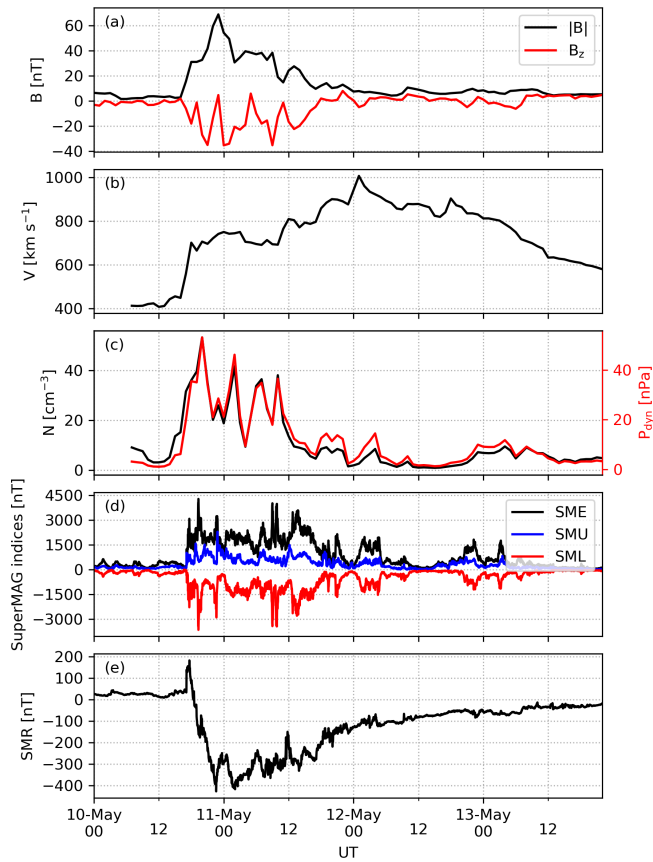
Figure 1. Driving and geomagnetic conditions during the Gannon Storm. **(a)** Interplanetary magnetic field magnitude (black) and B_z component (red). **(b)** Solar wind speed. **(c)** Solar wind density (black) and dynamic pressure (red). **(d)** SME (black), SMU (blue), and SML (red) indices. **(e)** SMR index.

in Fig. 1a. We can see that, around 16:00 UT on 10 May 2024, the IMF magnitude sharply increases from a few nanoteslas to the maximum of 69 nT at 23:00 UT. It remains significantly elevated throughout 11 May and does not decrease below 10 nT until the early hours of 12 May. During most of this time, B_z is predominantly southward (negative), reaching values as low as -35 nT at 21:00 UT on 10 May, 00:00 UT on 11 May, and 09:00 UT on 11 May. This strongly southward IMF component produces sustained magnetic reconnection at the dayside magnetopause, fuelling plasma convection in the inner magnetosphere and in the polar cap and subsequently leading to reconnection in the magnetotail associated with the injection of charged particles into the magnetosphere.

Figure 1b shows the solar wind speed. The data gap in the earliest hours of the considered time period is related to missing measurements. It can be seen that, at the same time as the IMF compression starts, the solar wind speed increases from about 400 km s^{-1} to over 700 km s^{-1} at the time of peak IMF field strength. The speed continues to increase until reaching

the maximum of 1006 km s^{-1} at 01:00 UT on 12 May, after which it gradually decays. It is still of the order of 600 km s^{-1} in the late hours of 13 May.

The solar wind density and dynamic pressure increase strongly in tandem on 10 May, reaching the maximum of 53 cm^{-3} and 53 nPa, respectively, at 20:00 UT (Fig. 1c). The decay of these two parameters happens by noon on 11 May, which is in agreement with the decay of the IMF structure and the strongest magnetic variability (SuperMAG electrojet (SME) index; see below) but is much faster than that of the solar wind speed, which remains high past 13 May.

To assess the geomagnetic response to these extreme driving conditions, we consider the provisional SuperMAG indices, derived from ground-based magnetometer measurements (Gjerloev, 2012). These indices have been retrieved at 1 min resolution. Figure 1d shows the SuperMAG electrojet (SME) index, together with its upper- and lower-envelope components, SMU and SML (Newell and Gjerloev, 2011). These indices provide a measure of the auroral electrojet intensity and are therefore used as a proxy for substorm activity. It is clear that an abrupt increase in substorm activity takes place shortly after the arrival of the solar wind disturbances: SME increases from under 200 nT to over 800 nT in the span of 2 min (between 17:05 and 17:07 UT on 10 May). SME continues to increase rapidly and reaches an initial peak of 3077 nT at 17:38 UT and a second peak of 4276 nT at 19:19 UT. Substorm activity remains extreme (i.e. SME > 2000 nT for a majority of the time) until $\sim$ 18:00 UT on 11 May and is elevated until about 06:00 UT on 12 May. We can see that, throughout the disturbed period, both SMU and SML exhibit elevated values (in absolute units), indicating recurring intensification in the westward and eastward auroral electrojets, respectively. To put this into perspective, we looked at the SME index values since the Halloween storms of 2003. We found that the SME exceeded 3000 nT during only 21 geomagnetic events between 20 November 2003 (excluded) and 31 December 2023. It exceeded 4000 nT only seven times during that 20-year period (and only twice during the previous solar cycle (SC24: 2008–2019): on 28 May 2011 and on 8 September 2017).

Finally, Fig. 1e shows the SuperMAG ring current (SMR) index (Newell and Gjerloev, 2012), which provides a measure of the ring current intensity and is hence used as a proxy for geomagnetic storm intensity. A very prominent storm sudden commencement (SSC; Akasofu, 2005) signature is visible, starting at 17:07 UT on 10 May and reaching a peak of 182 nT at 17:39 UT. Those two times are consistent with the solar wind dynamic pressure starting to increase, indicating a strong compression of the dayside magnetopause due to the arrival of the CME(s) on Earth. After the SSC signature, the SMR decreases rapidly until reaching a first minimum value of -427 nT at 22:36 UT on 10 May. A second minimum is attained around 2 h later (-417 nT at 02:06 UT on 11 May) during the geomagnetic storm's main phase. The

recovery phase is not fully over by the end of 13 May as the SMR values are still of the order of $-20\,\text{nT}$. To put this into perspective, the SMR went below $-200\,\text{nT}$ only eight times between 20 November 2003 (excluded) and 31 December 2023. It went below $-300\,\text{nT}$ only once (on 8 November 2004, meaning that this never happened during SC24).

3   Citizen science data collection and pre-processing

The Gannon Storm produced spectacular auroral displays that reached exceptionally low latitudes. This offered the opportunity for many people to witness and often photograph the northern and southern lights for the first time in their life. These observations bear the potential to be used as data to study this extreme event, supplementing optical data from scientific instruments which are mainly deployed in the polar regions (see, for example, Fig. 1 in Alfonsi et al., 2022).

To evaluate the potential of citizen scientist observations in providing insightful information on the Gannon Storm and its effects, we set up an online form enabling citizen scientists to report on their observations of auroral displays and technological disruptions. This survey was hosted on Google Forms and was distributed as widely as possible across online aurora-chasing communities. The form accepted answers between 18 May and 24 June 2024. The list of questions the survey contained is provided in Appendix A. Besides ours, similar initiatives have arisen from other teams who set up surveys to collect citizen science observations during the Gannon Storm and whose analysis is underway (e.g. Hayakawa et al., 2024).

By the end of the data collection period, a total of 696 reports had been submitted. Given that the data collection platform (Google Forms) did not enable the imposition of strong formatting constraints in the response fields, the data had to be pre-processed before carrying out the analysis. The pre-processing consisted of the following:

1. We harmonised all time zone information with respect to the Universal Time Coordinate (UTC) under the format "UTC±??" (e.g. UTC+00, UTC+12, UTC-06). Many responses referred to time zones either by their name (e.g. Mountain Daylight Time) or by the corresponding country or city (e.g. Paris time zone). Among the respondents, 109 indicated their observation time directly as UTC.

2. We harmonised all geolocalisation information under the format "latitude, longitude", with 0.01° precision (e.g. 48.12, −1.36; −36.84, 174.73). We retained this level of precision as it is sufficient for our purposes in this study. When no geographic coordinates were provided, we used the city; state, region, or province; and country information to search for an approximate geolocation. This was needed for 302 of the reports. In five cases, the provided geographic information was not sufficient (e.g. country only); these observations have hence been excluded from the analysis. The harmonisation to the desired format concerned the other 389 coordinates which were input with higher precision or with the degree, minute, and second format.

3. We corrected the dates which had been input in the American format (MM/DD/YYYY) or which had a typo in the year or month when the intended value was obvious. A total of 44 dates had to be corrected; in three cases, the intended value was unclear, and the corresponding reports have thus been excluded from the analysis.

4. We corrected the times which had not been entered in the 24 h format (i.e. which used a 12 h format, although no AM or PM information was appended). This ambiguity was easily spotted and corrected as no location from which the reports were issued could have possibly had visible aurora during daytime. There were 32 such corrections needed.

The pre-processed data used in this study are published as an openly available dataset (Grandin and ARCTICS collaboration, 2024). Note that, in order to protect the privacy of the survey participants, we downgraded the precision in their geolocalisation to 0.1° accuracy in this dataset. Moreover, the observations are not tied to the observers' names, but the citizen scientists who wished to be acknowledged by name in this paper are listed alphabetically in Appendix B.

In addition to the material collected via the survey form, observations made during the storm period were extracted through Skywarden's public data interface. Skywarden is a public, content-moderated observation system established by the Ursa Astronomical Association (Karttunen, 2021). Through its public application programming interface (API; Bruus, 2024), the data collected in Skywarden can be extracted in either HTML, CSV, XML, or JSON formats. This additional dataset from Skywarden contains 186 observations. Skywarden uses an online-form-based interface for gathering observations of different astronomical and atmospheric phenomena, including the aurora. The interface guides users to provide observation data directly in a defined and structured format.

Skywarden uses the ISO 8601 basic format for storing date and time information. Conversions from local to UTC time are done automatically by using Google's Time Zone API. In case user-set coordinate information is missing from an observation, Google's Geolocation API is used for retrieving the missing WGS84-format coordinates. Skywarden provides information on visually observed aurora colours and special aurora structures like SAR arcs, STEVEs, picket fences, dunes, etc. The identifications are checked by the moderator team before the material is published on the website. Because of the pre-existing mechanisms for securing ad-

equate data quality, no additional modifications were made to superstorm event citizen science data extracted from Skywarden.

4 Citizen science data analysis

4.1 Auroral observations

4.1.1 Overview of the reports

Figure 2 presents the locations from which citizen scientists reported aurora sightings and/or reported experiencing disruptions during the Gannon Storm. On the map, each black dot corresponds to an aurora sighting reported via the online survey. A total of 688 citizen scientists (out of the 696 respondents) indicated that they saw and/or photographed the aurora. The 42 red squares show where technological disruptions were reported via the online form. The blue triangles correspond to auroral observations logged in Skywarden; there are 186 of these. Most (170) of these latter observations are from Finland, but it is worth noting that the Skywarden data also include observations from Canada (4), New Zealand (3), the Netherlands (2), Sweden (2), Australia (1), Estonia (1), France (1), Germany (1), and the United States (1).

From the map, it can be seen that most reports come from three regions: Europe, North America, and Oceania. Only 10 reports come from other regions of the world: 4 from Chile, 2 from India, 2 from China, 1 from Namibia, and 1 from Argentina. This uneven coverage of the emerged land-mass can be explained by several factors:

1. *Collaborator network.* The survey was circulated by citizen scientists from our network of collaborators who are mainly able to reach observers from their own country.

2. *Language.* The survey was set up in English, making it less accessible to observers from non-English-speaking countries.

3. *Population density.* Some regions where few to no data points are available are sparsely populated (e.g. Patagonia, Russia, central Australia, Antarctica).

4. *Lack of darkness.* Since the geomagnetic storm took place less than 1.5 months away from the summer solstice in the Northern Hemisphere, high-latitude observations of the aurora were impeded by the lack of darkness (e.g. Alaska, northern Canada, Greenland, Iceland, northern Fennoscandia, Svalbard). The northernmost observation of the aurora during that storm reported in Skywarden was made just shy of 65° geographic latitude. In the most northerly observations, the Sun was only roughly 5° below the horizon.

The first two points, in particular, may explain the low number of reports from eastern Asia, while evidence of aurora

sightings is found in news articles from Japan (e.g. https://www3.nhk.or.jp/nhkworld/en/news/backstories/3308/, last access: 19 December 2024), China (e.g. http://en.people.cn/n3/2024/0513/c90000-20169018.html, last access: 19 December 2024), and Korea (e.g. Kwak et al., 2024).

While the limited coverage of reported observations of the aurora during the event does not enable us to obtain a comprehensive picture of the extent of the auroral oval, it is worth pointing out that, altogether, the citizen scientist reports provide information which is largely missing from scientific measurements. Indeed, most of the reports come from regions situated at mid-latitudes where scientific infrastructure targeting auroral studies (optical instruments, ionospheric radars, etc.) is sparse (e.g. Alfonsi et al., 2022). Besides, at high latitudes in the Northern Hemisphere, many of the optical instruments observing auroral emissions were not in operation during the storm since the background sky was not dark enough. This is the case for most optical instruments in the European sector. However, some instruments in North America, such as the THEMIS all-sky imager (ASI), TREx, MANGO, and others (e.g. Donovan et al., 2006; Liang et al., 2024; Bhatt et al., 2023), were able to record parts of the auroral activity. At some points during the geomagnetic storm, the auroral oval extended equatorward, beyond the field of view (FOV) of the TREx and THEMIS ASI networks (see Fig. 3). We will see below that scientific conclusions on this geomagnetic storm can be drawn from the citizen science data, even without sophisticated analyses of photographs taken by the citizen scientists.

4.1.2 Magnetic local time – geomagnetic latitude distribution of the observations

A simple, first result that can be obtained by analysing the collected citizen scientist observations is a measure of the auroral oval extent during the Gannon Storm. Figure 4 displays the locations from which citizen scientists reported seeing the aurora as a function of geomagnetic latitude (radial coordinate) and magnetic local time (MLT; angular coordinate). Such an approach to assess the auroral oval extent is similar to what projects such as Aurorasaurus (MacDonald et al., 2015) can routinely provide. The geomagnetic coordinates of observation sites have been calculated using the Python AACGM-v2 library (Burrell et al., 2020; Shepherd, 2014). Note that observations from the entire duration of the storm and from all regions are shown together in the figure.

In Fig. 4a, the observations are colour-coded to indicate the source (survey or Skywarden) and hemisphere to which they correspond. Clearly, most of the aurora observations took place in the evening sector, with the majority of points being confined to 18–00 MLT. Rather than being an indication that the auroral activity was more intense in the evening sector than in the morning sector, this asymmetry can be explained by human behaviour – citizen scientists are more prone to viewing the aurora in the evening hours rather than

Citizen scientist reports on the 10 May 2024 superstorm
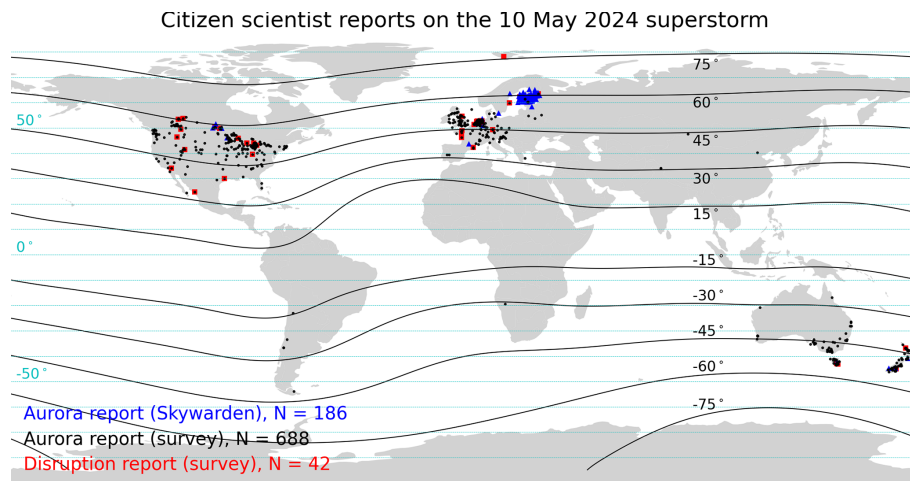
Figure 2. Map of the received reports on aurora sightings from Skywarden (blue triangles) and our survey (black dots) and on experienced disruptions from the survey (red squares) during the Gannon Storm. The black isocontour lines indicate selected geomagnetic latitudes, and the thin cyan lines show the geographic latitude grid.
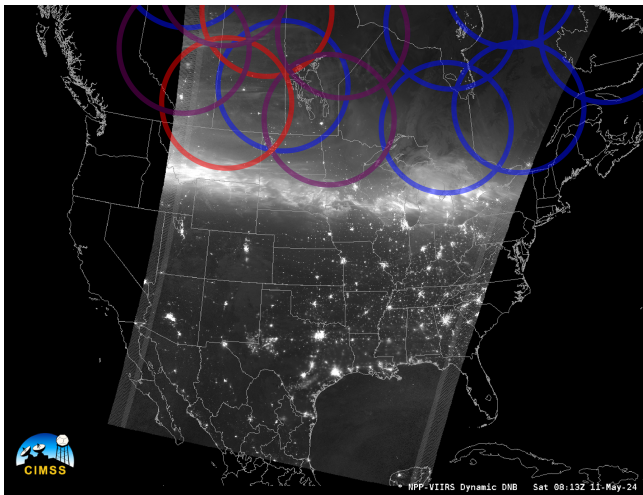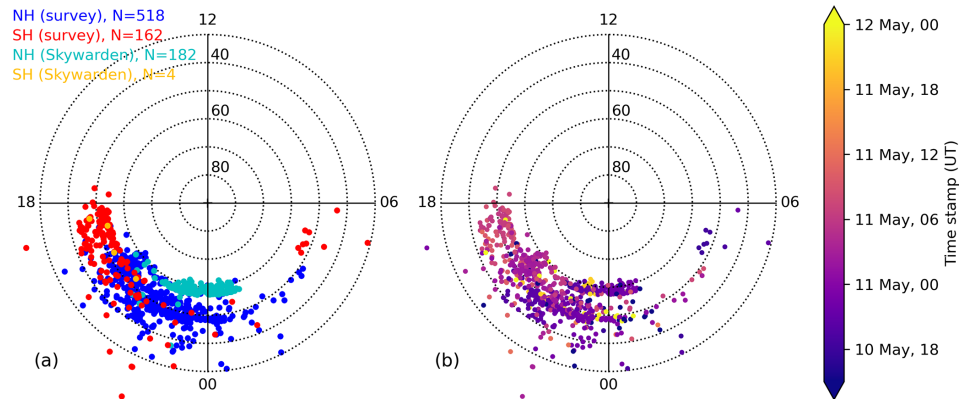

Figure 3. Image from the Visible Infrared Imaging Radiometer Suite (VIIRS) Day/Night Band (DNB) onboard the Suomi NPP satellite, showing a portion of the aurora over the central United States. Data were captured during the geomagnetic superstorm at 08:13 UT on 11 May 2024. FOVs of THEMIS (blue) and TREx (red) ASIs are overplotted. Co-located TREx and THEMIS ASIs are shown in purple.

most-equatorward report of aurora observation comes from San Pedro de Atacama, Chile, at a geomagnetic latitude of $-14.5°$. However, at such a low latitude, it is likely that the cause for the observed red emissions was an unusually bright airglow display, presumably linked to the extreme geomagnetic activity. Nonetheless, the auroral oval expansion was exceptional during the geomagnetic storm. This is supported by Fig. 3, which shows an extended portion of the auroral oval in the Northern Hemisphere at 08:13 UT on 11 May 2024, when storm and substorm activity was very high (see Fig. 1d–e). The aurora was overhead of $\sim 50°$ geomagnetic latitude at that time.

We can obtain a more detailed view on the latitudinal extent of the auroral oval during the storm by considering Fig. 4b, where the data points are colour-coded as a function of their corresponding time stamps between 18:00 UT on 10 May 2024 and 12:00 UT on 12 May. Observations beyond this time window (31 earlier, 11 later) are shown in the figure, with the colour corresponding to the boundary of the time interval. From the colour of the points, we can conclude that the most equatorward sightings of the aurora took place during the late hours (in UT) of 10 May 2024, with clusters of dark-blue dots around 40° geomagnetic latitude in the pre-midnight sector and around 50° latitude near the dawn sector. The aurora was also visible at high latitudes (around 60°) near midnight, indicating that the auroral activity was spanning across at least 20° in geomagnetic latitude. Purple dots (corresponding to 00:00–06:00 UT on 11 May) are mainly confined to 50–60° geomagnetic latitude, consistent with a period of lower (although still above 1500 nT) SME index values (see Fig. 1d). During the hours spanning around 12:00 UT on 11 May, we mostly see near-dusk observations from the Southern Hemisphere as Australia and New Zealand were the only places with suitably dark conditions. Reports

waking up shortly after midnight to observe it in the morning. However, we note that a non-negligible number of observations were made between 00 and 06 MLT. Moreover, one can notice that dusk (18–20 MLT) and dawn (04–06 MLT) observations all came from the Southern Hemisphere; this is because of the near-summer conditions in the Northern Hemisphere leading to short nights. In terms of geomagnetic latitude, we have most observations spanning from 40 to 60° and a significant number coming from lower latitudes. The

Figure 4. Distribution of aurora sightings during the Gannon Storm as a function of geomagnetic latitude and magnetic local time. The distribution is shown as a function of **(a)** data source and hemisphere and **(b)** observation time stamp. NH: Northern Hemisphere; SH: Southern Hemisphere.

of aurora sightings from geomagnetic latitudes as low as 40° came from this region as SME peaked above 3000 nT. Finally, during the late hours of 11 May and beyond (yellow dots), the few reports of aurora that were made come from 50–60° geomagnetic latitude, again consistent with subsiding auroral activity as measured by the SME index.

The data shown in Fig. 4 do not strictly give the geomagnetic latitude at which auroral emissions occurred. Indeed, without knowing the elevation of the aurora from a given observation place, there is an uncertainty with regard to the geomagnetic latitude at which the auroral emissions take place. Assuming minimum elevations of 5° above the horizon for the reported auroral sightings and considering 250 km (110 km) to be the altitude of the red (green) emissions, the oval boundary can be inferred with an uncertainty of ±1284 km (743 km) at best, which corresponds to $\pm11.5°$ ($\pm6.7°$) in geomagnetic latitude. Despite those rather large uncertainties, this is still a valuable quantitative estimate of the equatorward boundary of the auroral oval to supplement the few available scientific-grade observations obtained during extreme events such as the 10 May 2024 geomagnetic storm.

4.1.3 Reported auroral colours

Citizen scientists can also report the colours observed in the aurora, which is scientifically valuable information. Figure 5 shows histograms of the reported colours as a function of geomagnetic latitude, both as appearing in pictures (Fig. 5a) and as visible to the naked eye (Fig. 5b). We consider four auroral emission colours in this study: red; green; blue; and purple, pink, and/or magenta. While the first three typically come from the atomic oxygen 630 and 558 nm emissions and the molecular nitrogen ion 428 nm emission, respectively, the purple, pink, and/or magenta colours generally result from a mix of emissions (Sandholt et al., 2002) or can be the result of blue emissions seen in twilight conditions (see below).

Comparing the two panels of Fig. 5, we can see that the four considered colours were reported by the observers, both in pictures and as seen with the naked eye. This suggests that the auroral displays were not only reaching exceptionally low latitudes but were also of exceptional brightness since colours generally cannot be distinguished by the naked eye when the aurora is dim. The human eye's sensitivity to colour is maximised at around 530–560 nm (Malacara, 2011), which makes the visual observations of red colours exceptional (Schnapf et al., 1987). A very large number of reports indicated red emissions seen with the naked eye, which implies very bright auroral displays during the geomagnetic storm.

Focusing on the latitudinal distribution of the observed colours, one can see that a wide range of geomagnetic latitudes have reports of all four colours. It is of particular interest to note that green emissions were seen down to about 38° geomagnetic latitude and were photographed down to about 35°. This is very unusual as, when the aurora reaches mid-latitudes, it is mainly red emissions at high altitudes that are observed (Green and Boardsen, 2006). Red (and purple, pink, and/or magenta) auroras were seen and photographed by a few observers below 30° geomagnetic latitude and even down to 14.5° geomagnetic latitude, although, as mentioned above, in this extreme case, this was likely to be strong airglow; this is consistent with the fact that only the uppermost part of the aurora could be seen just above the poleward horizon for those observations, and the upper part of the red emission can be strongly enhanced during geomagnetic storms driven by dense solar wind (Kataoka et al., 2024). The low latitudes for auroral observations are beyond the NOAA geomagnetic storm category G5 definition, which says that auroras are typically seen down to about 40° geomagnetic latitude (see https://www.weather.gov/media/publications/assessments/SWstorms_assessment.pdf, last access: 19 December 2024).
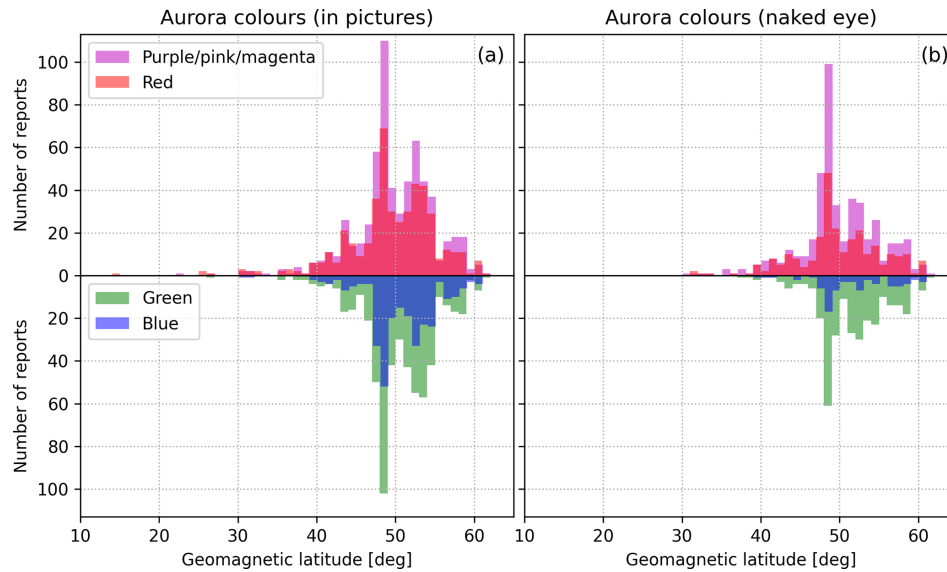
Figure 5. Reported colours of the aurora **(a)** in pictures and **(b)** visible to the naked eye during the Gannon Storm as a function of geomagnetic latitude. The data from both hemispheres are blended together.
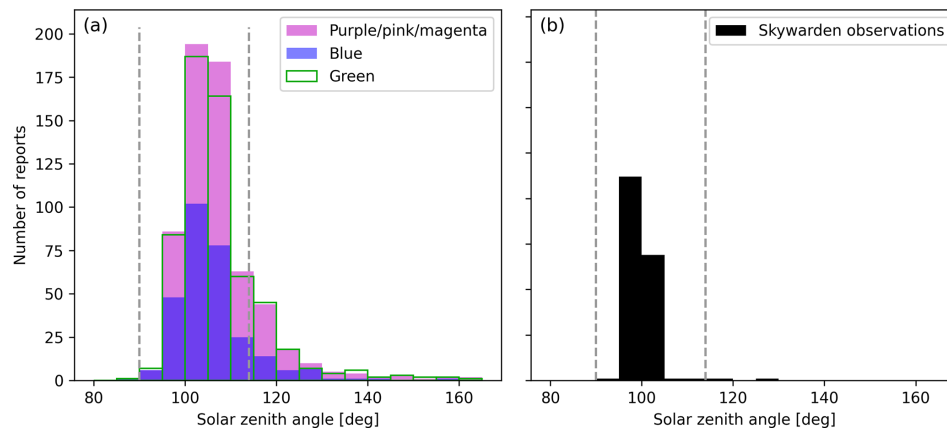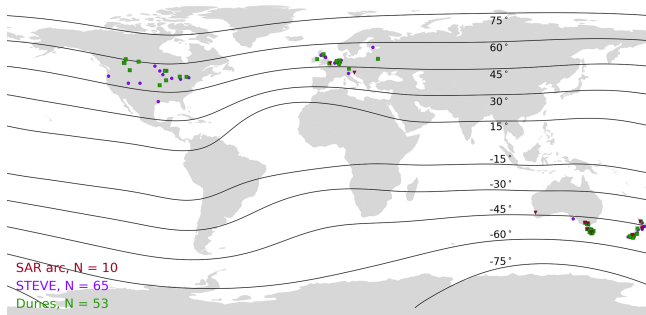

Figure 6. Distribution of solar zenith angle values **(a)** corresponding to the observation of purple, pink, and/or magenta; blue; and green auroral emissions in the survey reports and **(b)** in Skywarden observations. The vertical dashed grey lines indicate solar zenith angle values of 90 and 114°, corresponding to solar elevations between 0 and −24°.

A striking feature visible in Fig. 5 is that a large number of observers reported red and purple, pink, and/or magenta aurora, both in pictures and as naked-eye observations. While the intense red aurora suggests that large fluxes of low-energy ($\ll 1$ keV) electrons depositing their energy above about 200 km were precipitating during the event (Fang et al., 2010), the purple, pink, and/or magenta emissions can result from two main mechanisms. First, such colours can be seen in the E-region aurora in the presence of ~ 1–10 keV electron precipitation, when emissions from molecular nitrogen produce pink hues in the aurora (Whiter et al., 2023). Second, similar colours can be obtained at high altitudes (above about 150–200 km) via resonant scattering of sunlight by N_2^+ excited in presence of low-energy electron precipitation

and ion upflow (Bates, 1949; Broadfoot, 1967). This leads to blue (428 nm) emissions, which appear to be purple or pink against less dark night skies. This process takes place when the upper atmosphere is sunlit. Shiokawa et al. (2019) showed that such conditions are met when the solar elevation at the observation site is higher than −24° (i.e. less than 24° below the horizon), which corresponds to solar zenith angles between 90 and 114°. At −24° solar elevation, the shadow of the Earth reaches about 600 km altitude (without accounting for sunlight scattering in the upper atmosphere).

To investigate the origin of the blue and purple, pink, and/or magenta aurora reported by the citizen scientists in the survey, we calculate the solar zenith angle at the time and location of the observations comprising these colours.

Figure 7. Map of the reports of sightings of SAR arcs (red), STEVEs (purple), and dunes (green).

Figure 6a shows the solar zenith angle distribution of these observations. Two vertical dashed lines indicate solar zenith angles of 90 and 114°, between which the resonant scattering mechanism in the sunlit upper atmosphere (at ∼ 150–400 km) can take place. One can see that the large majority of the reported blue and purple, pink, and/or magenta auroras are associated with solar zenith angles within this range, suggesting that these colours likely find their origin in the resonant scattering mechanism, hence requiring low-energy electron precipitation (below 1 keV). Resonant scattering at the top part of the atmosphere allows the vivid pink emission to be seen from a distance. However, this observation alone does not exclude possible higher-energy electron precipitation during the superstorm. The higher-energy electrons would rather result in green emissions at lower heights, which may be blocked by the horizon for individual observers viewing from a distance. The fact that the solar zenith angle distribution of green aurora (unfilled green bars) is very similar to that of purple, pink, and magenta aurora supports the hypothesis that the kiloelectronvolt range of electron precipitation was also taking place and was visible to the observers closer to the electron precipitation region. This is in agreement with results presented by Foster et al. (2024), who used total electron content measurements along with auroral images in the North American sector during the Gannon Storm.

While information on the colour of the aurora is not systematically provided in Skywarden observations, many reports and uploaded pictures corresponding to the Gannon Storm contain spectacular displays of blue, purple, and pink aurora. Figure 6b shows the solar zenith angle distribution associated with the Skywarden observations. It is clear that almost all observations were made during conditions that made it suitable for the daylight resonance scattering mechanism to take place. This makes sense since most of the Skywarden observations are from Finland, where darkness was barely sufficient to see the aurora during the geomagnetic storm.

4.1.4   Special auroral forms in the reports

Finally, among the questions asked via the online survey, one was about the observed auroral forms during the event. In the absence of detailed guidance given to citizen scientists regarding the identification and logging of specific auroral forms, analysis of the obtained responses would prove to be cumbersome and would likely provide little insight. However, we can look at a few optical features which are so peculiar that the risks of misidentification are low. Figure 7 shows the locations at which STEVEs (in purple), dunes (in green), and SAR arcs (in red) were spotted during the Gannon Storm. With this nomenclature being very specific, it is likely that only citizen scientists already familiar with those phenomena ventured to indicate their presence in the night sky during the event. Overall, 65 reports bear a mention of STEVEs, 53 reports indicate the presence of the dunes, and 10 citizen scientists report seeing a SAR arc. One can note that the reports almost exclusively originate from regions where active groups of aurora chasers are present and organised as communities on social media: Canada and the northern United States, the United Kingdom, the Netherlands, Tasmania, and New Zealand. This is consistent with the above statement that only citizen scientists familiar with the concepts of STEVEs, dunes, and SAR arcs could provide such identifications. While the map given in Fig. 7 cannot provide a comprehensive overview of all the regions where these phenomena appeared and while it has not been possible to systematically validate the identifications, it gives a promising indication concerning possible data sources in case one would like to investigate either of these processes in more detail.

4.2   Disruptions in human-made infrastructure

Although the number of disruptions reported via the survey is fairly low (42), it is nonetheless interesting to investigate the types experienced by the citizen scientists during the geomagnetic storm. Table 1 presents the main types of disruptions reported. Since some citizen scientists reported several disruption types, the sum of the numbers in the right-hand column (46) exceeds the total number of reports (42). More than half of the reports mention issues with geolocalisation services, indicating inhomogeneities in the ionospheric E- and F-region electron densities, producing scintillation of GNSS signals. Such inhomogeneities can be produced by instabilities arising from electron density gradients or turbulence, which can result from particle precipitation (e.g. Enengl et al., 2024). About a quarter of the reports indicate problems with network or connectivity; free-text descriptions mention either mobile network or home internet issues. Only a few reports concern disruptions related to electricity (unstable power or power cuts), which may tell us about the resilience of our power grids and/or about the fact that this

Table 1. Main types of disruptions during the Gannon Storm as reported by citizen scientists.

Disruption type	Number of reports
Geolocalisation problem	22
Network or connectivity problem	11
Unstable power	8
Power cuts	5

Figure 8. (a) Distribution of reported disruption times from the survey. (b) SMR index.

storm did not drive extreme current variability in the E region.

It is also instructive to look at the times when disruptions were experienced. Figure 8a shows the distribution of the disruption times. We see that disruptions start after 12:00 UT on 10 May and that the number of reports peaks during the late hours of that day. A second peak of disruption reports takes place after 12:00 UT on 11 May. In Fig. 8b, we reproduce the SMR time series (same as in Fig. 1e); we can see that these two peaks correspond well with abrupt decreases in the SMR index as the geomagnetic storm activity was increasing. However, since the overall number of reports is low, one cannot exclude the possibility that the apparent anticorrelation between the number of reports and the SMR index is coincidental. This nonetheless suggests that developing tools to collect disruption reports from citizen scientists during geomagnetic storms could prove to be important in assessing space weather effects on daily life.

5 Discussion

5.1 Spontaneously collected data outside of an observation campaign

We have seen that data collected from citizen scientists can provide insights into space weather events, especially when they are strong enough to affect densely populated mid-latitude regions. In a noteworthy recent publication on the Gannon Storm, Spogli et al. (2024) showed examples of aurora observations from the general public in the form of a map shared on Twitter/X, along with individual photographs from observers based in Italy and shared via Instagram. They hence highlighted the opportunity given by the superstorm to engage in communication with the public, which was also one of the motivations of our study.

The first point to highlight concerning our study is that the collected data were obtained a posteriori as opposed to being gathered via a coordinated campaign. This means that the number of reports we obtained could have been significantly greater if there had been a planned campaign of auroral observations, including basic training for citizen scientists to know in advance what to look for and how to take pictures of the aurora. Recently, the ARCTICS collaboration released its *Auroral Field Guide and Handbook for Citizen Science* (Herlingshaw et al., 2024) to partly address this challenge.
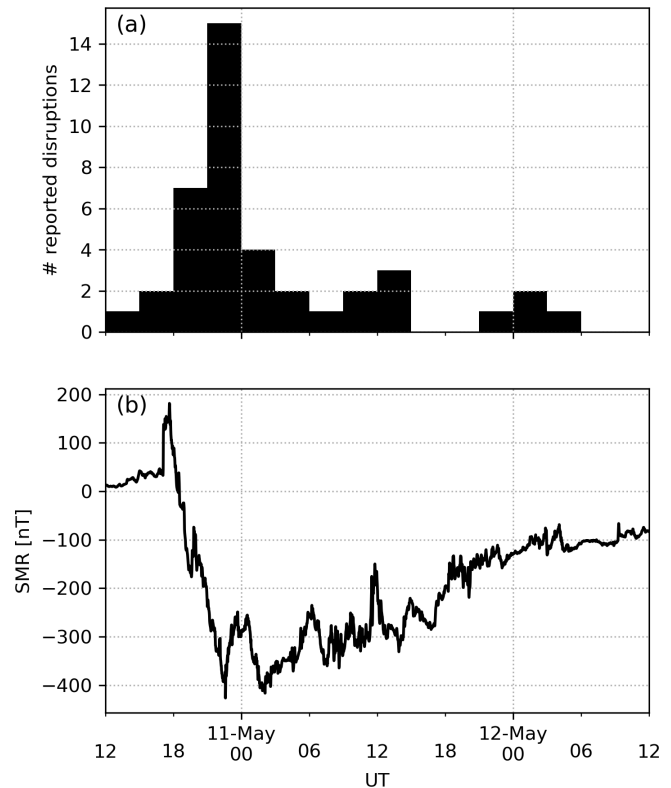
Fortunately, the event was forecast several days in advance, and citizen scientists, photographers, and the general population had been alerted through aurora networks, as well as through mainstream news outlets. Therefore, this event was observed by many people. As many smartphones now have high-quality cameras, including night modes with longer exposure times, this made it possible for many observers to detect the full range of green, red, blue, and pink emissions which are not typically easy to discern with the naked eye.

5.2 Opportunity to develop new methods for the analysis of citizen scientist images

While, in this study, we did not request aurora pictures from the citizen scientists and mainly presented an analysis of the collected metadata, one should bear in mind that, based on the reports logged via our survey, there exists a large number of auroral images by citizen scientists from all around the world for this exceptional event. This opens possibilities for future analysis of those images in a quantitative manner.

For instance, new image processing methods can enable the conversion of the red, green, and blue (RGB) pixel values from a raw photograph into scientific parameters. Recent simulations of the full synthetic spectra of the aurora performed with the Transsolo code (Lummerzheim and Lilensten, 1994; Lilensten and Blelly, 2002) allow the estimation

of the mean energy of precipitating particles from the ratios between the RGB brightness values. Preliminary calculations using the MATLAB function spectrumRGB between 380 and 900 nm (MATLAB Central, Mather, 2024) yield a dominant level in the red channel for low-energy precipitation (in the 100 eV range), comparable RGB levels for medium energies (a few kiloelectronvolts), and a dominant level in the green channel for higher energies (10 keV or more). These colour ratios are considered when looking at the zenith or near-zenith elevations, which provides an altitude-integrated view. When looking at low elevations, each pixel from the detector contains a signal originating from a limited altitude range, which needs to be accounted for in the analysis.

In the case of the May 2024 superstorm, the citizen scientist reports suggest that a large part of the pictures show predominantly red emissions, which implies that a significant fraction of the precipitating electrons have energies below 1 keV. Applying a systematic analysis of the citizen scientists' images could provide estimates of the precipitating electron mean energies at different times and places during the superstorm, and more complex methods such as tomographic reconstructions (Robert et al., 2023) could be envisaged and tested.

5.3   Limitations of the study and lessons learnt

Among the main limitations of our approach to collect the citizen science data is the difficulty in validating data accuracy. Given that the reports were manually logged by citizen scientists with little guidance and few formatting constraints, a non-negligible number of corrections had to be made, especially to observation times, time zones, and geolocalisations (see Sect. 3). Besides this, some of the collected data proved to be difficult to analyse and did not yield any insightful results. For instance, the question about the location of the aurora in the sky with respect to the observer (see Appendix A) contained possible answers (polewards, equatorwards, near zenith, everywhere) that were likely to be too subjective or too difficult to remember afterwards. Likewise, the question about auroral-form identification (quiet arc, moving or active arc, spirals or swirls, nearly vertical beams or pillars, coronas, blobs or patches, diffuse aurora, pulsating aurora, dunes, STEVEs) proved to be too technical for many citizen scientists, a significant fraction of whom saw the aurora for the first time in their life during the studied superstorm.

This underlines the necessity for clearer and more accurate directions for citizen scientists responding to forms such as the one distributed. There should also be an effort to widely distribute accessible documentation for citizen scientists to refer to when trying to identify auroral forms. The ARCTICS Handbook (Herlingshaw et al., 2024), released a few months after the Gannon Storm occurred, contains guidance and advice on how to take auroral photographs for scientific purposes and how to handle the associated metadata (e.g. time, location, camera settings). Besides, training sessions for as-

piring citizen scientists could be another way to improve the quality and accuracy of the collected data in view of more detailed studies of auroral processes. While the objective of the online survey was not to directly collect the images taken by citizen scientists, it is worth pointing out that dedicated platforms such as Skywarden can be readily used for such purposes as they are designed to guarantee good practice in terms of data archival, data quality control, content verification, data reusability and/or access, credit attribution, and auroral-form classification.

Concerning the reported disruptions in human-made infrastructure, using an online survey or social media posts to collect data comes with even more shortcomings. First, the causality link between a disruption experienced by a user and space weather activity cannot be demonstrated. Although the temporal distribution of the reports shown in Fig. 8a is consistent with the SMR index variations, one cannot exclude that there may be a bias in reporting disruptions that occurred at the same time that strong auroral activity was present, while similar disruptions occurring during geomagnetically quiet times would be left unnoticed (illusory correlation). Second, some of the reported disruptions (e.g. network problems) can have multiple causes, and without being able to investigate each individual case in detail, it is impossible to confirm a possible geomagnetic origin for it.

Nevertheless, one should not hastily discard the potential of gathering disruption reports from citizen scientists as this can provide large amounts of data that give insight into space weather effects and that can aid in evaluating their economic cost. For instance, according to the Solar Influences Data Analysis Centre from the Royal Observatory of Belgium, some GNSS-based tools for aviation were not working properly for several hours during the Gannon Storm, affecting aircraft navigation (https://www.sidc.be/article/extremely-severe-geomagnetic-storm, last access: 19 December 2024). Besides this, in Canada and the northern United States, there have been reports of farmers being unable to use navigational systems on which their farming equipment rely (e.g. https://www.cbsnews.com/minnesota/news/solar-storms-cause-gps-outage-is-tractors-planting-season/, last access: 19 December 2024); a few responses to our survey contained similar statements as free-text comments. For some, this affected the accuracy of the planting of their crops right at the peak of the planting season, which may yield a loss in productivity. Evaluating the economic cost of the superstorm for the farming industry and other sectors could prove to be useful in devising mitigation strategies in future. This calls for setting up adequate tools to facilitate and systematise reporting so that the collected data can easily be used in quantitative studies.

5.4 Going further: extreme storm effects from publicly available data

More generally, both citizen science and also publicly available data could be more systematically utilised to infer scientific results on space weather effects during extreme geomagnetic events like the Gannon Storm. For instance, orbit data of thousands of satellites can be retrieved via services such as CelesTrak (https://celestrak.org, last access: 19 December 2024). When a strong geomagnetic storm takes place, ion–neutral frictional (Joule) heating takes place in the ionospheric E region within the auroral oval, leading to vertical expansion of the upper atmosphere (Palmroth et al., 2021). As a result, low-Earth-orbiting spacecraft experience increased drag, which speeds up their altitude loss. Figure 9 shows the semi-major axis altitude of the orbits of four selected satellites between 3 and 22 May 2024. The satellites are, by decreasing altitude, AMICal Sat (NORAD ID no. 46287); the International Space Station (ISS); AALTO-1 (NORAD ID no. 42775); and AIS & APRS & ARIS & R/B (NORAD ID no. 44104). The time interval indicated with grey shading, from 16 UT on 10 May until the end of 13 May, corresponds to the superstorm period.

The orbit data of the four spacecraft exhibit clear signatures during the superstorm as their semi-major axis altitudes dropped noticeably faster than their quiet-time decay rate shortly after the beginning of the event. To estimate the altitude loss due to the superstorm, we performed a linear fit of the pre-storm data, giving the average quiet-time decay rate of the altitude of each spacecraft in early May 2024 (numbers indicated in blue in the top-right corner of each panel). The linear fits, extrapolated to the superstorm period and until the end of the displayed time interval, are shown with dotted blue lines. We can estimate the altitude loss resulting from the geomagnetic activity during the superstorm by comparing the measured satellite semi-major axis altitude at the end of the storm period with the extrapolated value at that same time. This yields a superstorm-associated altitude loss of 717 m for AMICal Sat, 256 m for the ISS, 1131 m for AALTO-1, and 2091 m for AIS & APRS & ARIS & R/B. A recent study by Parker and Linares (2024) showed that several thousands of low-Earth-orbiting satellites performed manoeuvers simultaneously after the superstorm to compensate for the altitude loss, which is unprecedented.

We can see that the effect increases as we consider spacecraft orbiting at lower altitudes, which is a result of the density structure of the upper atmosphere following an exponential decay with altitude. The ISS is an exception to this trend; although its size makes it prone to atmospheric drag, the inclination of its orbit (51.6°) confines it to low and middle latitudes. This is contrary to the other three satellites, which are on polar orbits and hence flew through the entire auroral oval, experiencing enhanced drag along greater portions of their orbits. Nevertheless, it is known that the effects of space weather on satellite drag are not limited to
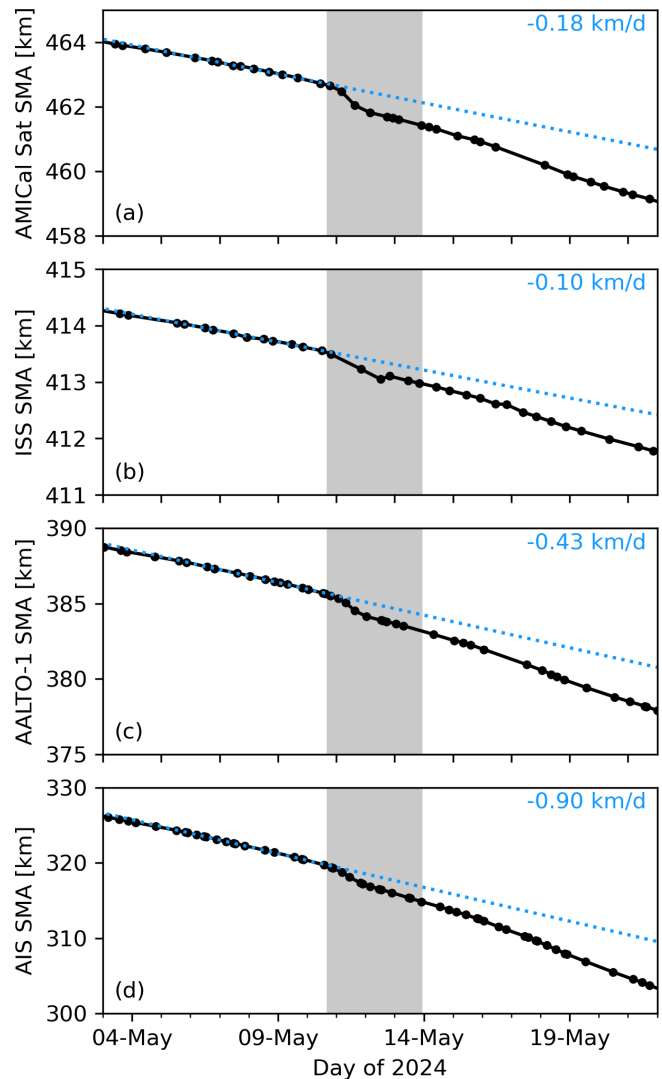
Figure 9. Time evolution of the semi-major axis (SMA) altitude of selected spacecraft on May 2024. The data are shown for **(a)** AMICal Sat (NORAD ID no. 46287), **(b)** the International Space Station (ISS), **(c)** AALTO-1 (NORAD ID no. 42775), and **(d)** AIS & APRS & ARIS & R/B (NORAD ID no. 44104). The grey-shaded area indicates the superstorm period. The dotted blue lines indicate the extrapolation of the SMA altitude based on the pre-storm altitude loss rate, given in the top-right corner of each panel for the corresponding spacecraft.

those in polar orbits as local heating within the auroral zone can be redistributed polewards and equatorwards via upper-atmospheric dynamics (Lu et al., 2016) and hence affect the mass density at mid-latitudes. Simulations from the empirical US Naval Research Laboratory's Mass Spectrometer and Incoherent Scatter radar Extended model (NRLMSISE-00; Picone et al., 2002) indicate significant atmospheric neutral density enhancement at 400 km altitude during the Gannon Storm, also affecting mid-latitudes (Parker and Linares, 2024), supporting this interpretation.

However, in the case of the Gannon Storm, it cannot be excluded that direct heating affected the most poleward portions of the ISS orbit, given that the aurora was seen from locations significantly equatorward from 50° geographic latitude (see Fig. 2). This would be consistent with neutral temperature enhancement observations made by the Global-scale Observations of the Limb and Disk (GOLD) satellite during the event (Evans et al., 2024). In fact, few data on the width of the auroral oval exist for extreme events. While a previous study by Case et al. (2016b) showed that citizen scientist reports of aurora sightings via Aurorasaurus were overall consistent with view line predictions by the OVATION Prime model (Newell et al., 2014), this result held for moderate to strong geomagnetic activity (Kp ≤ 7). For extreme events such as the Gannon Storm, models do not predict as broad an oval as what can be inferred from our citizen scientist reports (e.g. Sigernes et al., 2011; Newell et al., 2014; Blake et al., 2021; Spogli et al., 2024). This highlights the importance of considering citizen science observations to supplement and improve auroral oval prediction models. Such endeavours would prove to be crucial not only to better forecast auroral visibility when extreme events are expected but also to evaluate more finely the extent of the areas which may be affected by space weather events, both on the ground and along satellite orbits.

6 Conclusions

We presented a study of the auroral observations and disruptions experienced during the Gannon Storm based on citizen scientist reports gathered via an online survey. A total of 696 observers from around the world submitted responses, which enabled us to get insights into the effects of the superstorm that could not be obtained with the existing scientific infrastructure alone.

Lessons learnt from this study can be summarised as follows:

1. Communities of aurora chasers or enthusiasts following dedicated social media pages are likely to actively get involved in citizen science, even when having had no prior experience with it. Although few people consider themselves to be avid citizen scientists, the general public will respond to a request from a trusted leader or group that they follow, especially when there is an incentive such as getting their observation reported on a map or analysed in a study. This underlines the importance of collaborating with community managers or ambassadors who can act as intermediaries between academics and the general public.

2. The collection and pre-processing of citizen science data poses challenges, such as outlining adequate guidance and background information for citizen scientists to be able to answer any questions asked of them and constraining the format in which data are logged. This highlights the need for openly available documentation for citizen scientists, as well as the crucial role of data collection platforms managed according to professional data collection practices, such as Skywarden.

3. The analysis of the collected aurora sightings during the Gannon Storm showed that the auroras were visible down to beyond 40° geomagnetic latitude, with a few reports as low as below 30°. Auroral oval boundary models are currently not capable of accounting for observations at such low geomagnetic latitudes during extreme events.

4. The colours of aurora reported by the citizen scientists included unusually bright reds, pinks, and blues, even visible to the naked eye. This suggests that large fluxes of low-energy (< 1 keV) electron precipitation were dominant during those phases of the event. The pink hues can be explained by high-altitude blue emissions in the sunlit upper atmosphere.

5. Only a few reports regarding disruptions were made, yet their temporal distribution matched well with the geomagnetic activity level as measured by the SMR index. The main types of experienced disruptions were issues with geolocalisation systems, networks, and power. Dedicated tools to collect reports on human-made infrastructure disruptions during geomagnetic events could prove to be valuable in future cost assessment due to space weather disturbances.

The Gannon Storm is exceptional in terms of aurora reports, especially those from low latitudes beyond the prediction capacity of current auroral oval models. Besides, perturbations of GNSS signals were reported from various latitudes, and low-Earth-orbiting satellites lost up to 2 km in their semi-major axis altitude due to the geomagnetic activity. While, thankfully, no major power outage or spacecraft losses were reported during this superstorm, presumably because of the predominantly low-energy particle precipitation, major space weather events with different driving conditions could have much more devastating consequences. Therefore, it is crucial to make use of all available data to ensure that the effects and processes taking place at latitudes not covered by scientific instruments are measured and characterised. Thanks to the enthusiasm of citizen scientists all over the world, such data can be collected during future events. Improving the citizen science data collection and management methods is paramount to enable more quantitative studies and to monitor the Earth environment.

Appendix A: Survey questions

The following is the list of questions citizen scientists answered in the survey.

- Name.

- Do you want your name to be acknowledged in the report?

- Email address (if you want to be updated on the report).

- Location (closest town or city; state, region, or province; and country).

- Geographic (GPS) coordinates, if you know them (e.g. 38.898, −77.036).

- Did you experience any disruption (e.g. geolocalisation issues, power cuts, flickering lights) during the storm?

  - *If answered yes to the above question:*
  - Date when you experienced the disruption.
  - Approximate time when you experienced the disruption.
  - Time zone in which the above time is given.
  - If you experienced disruptions several times during the storm period, you can list them below.
  - What kind(s) of disruption(s) did you experience?

- Did you see the aurora during this event?

  - *If answered yes to the above question:*
  - Date when you saw and/or photographed the aurora.
  - Approximate time at which you saw and/or photographed the aurora (if you stayed for an extended period, indicate the starting time).
  - Time zone in which the above time is given.
  - If you saw and/or photographed the aurora several times during the storm period, you can list them below.
  - Location where you saw the aurora (city; state, region, or province; and country or GPS coordinates)
  - What type(s) of aurora(s) did you see?
  - What colours of aurora did you see (naked eye)?
  - What colours of aurora did you capture (in pictures)?
  - Location of the aurora relative to you.

Appendix B: List of the data providers (online survey)

The data presented in this study were collected via an online form between 18 May and 24 June 2024. A total of 696 citizen scientists filled in a report on their observations during the superstorm, among whom 195 wished to remain anonymous. The 501 contributors who consented to being acknowledged by name are as follows: Ada Verbree-Guijt, Adam Meyer, Adeline Sarah Jebaraj, Adriana Kasel, Aishath Zahwa, Aishwerya Kapoor, Akshatha Gopinath, Alan Dyer, Alasdair Taylor, Alessandro, Aletta Elders, Alex Daykin, Alexander, Alexander, Alexis Clift, Alfredo Juarez, Alison Thomass, Allison Mills, Amanda, Amanda, Amanda Hawn, Amrit Grewal, Amy Hester, Amy Willis, Anais Giblot-Ducray, Andrea McArthur, Andreas Milanese, Andrew Cadie, Andrew Vis, André Magalhães, Angela Gnewikow, Angela Nicol, Angela Robinson, Anke Verhaegen, Ann E. Johnson, Ann Towers, Anna Gottlieb, Anne Rodriguez, Anne Verzijl, Anne-Sophie Bescond, Anouk Vorselman, Anoula Voerman, Arjan, Arjan Kievits, Arjan de Jong, Arlene Oetomo, Arnaldo Lopez, Ashley Elsworth, Astrid Broere, Audrey Todd, Austin E., Ayla Embil, B. Wassenaar, Barbara koster, Barend (Barry) Becker, Bas Zonneveld, Benjamin Barakat, Berna van Tol, Beth Mason, Bo Krause, Boris Baloh, Brandon Walsh, Brighton Seeley, Bryn Jones, Candace Montgomery, Carlo W., Carmen Varela, Carola van Hof, Carole Sneed, Caroline Meijer, Caroline Whittaker, Carrie Bastyr, Centro de Instrumentación Científica de UNACH, Charles Le Béhot, Charlotte Bridgett, Charmayne, Chloe Jellis, Chrissey, Christa Creech, Christian Harris, Christina, Christopher Jones, Christos Doudoulakis, Chuck Benz, Claire Doran, Claudia Koekoek, Claudia Meulenbelt, Clément, Cole Gifford, Colette Dupont, Colin Legg, Constance Lewis, Corine, Corinna Zeller, Corné Ouwehand, Cory Goings, Croydon Hall, Daan van Laar, Dai Jianfeng, Daisy, Dakota Snider, Dale Turner, Dale Weigt, Dalton Mojica, Damijan Prosenak, Dan Nigro, Daniel Fernandes Gama, Danielle ODea, David Hunter, David Lusby, David Rius Serra, David Roberts, David Smith, Davide Maligno, Dawn Burbidge, Deb Angel, Deb Dennison, Deb Wiensch, Debbie, Debra Pierrehumbert, Diana Marell, Diane Chandler, Diane Thompson, Dmitri Kamenetsky, Donna Lach, Dorien ten Hulscher, Doug Cottrell, Eero Karvinen, Elan Azriel, Elizabeth Miller, Elizabeth Palmer, Eman Dannawey, Embla Wihk, Emily Donley, Emma Bruus, Enrique Carrasco, Entoni Novosel, Enzo Carlos, Eren Matthews, Eric, Eric B., Erin Dijkstra, Ernstjan Penninkhof, Erum Tanvir, Esther, Eva van Gent, Ewan Kane, Ezgi Gülay, Farin Drewes, Federico Butac, Ferdie, François Le Béhot, Freja van der Niet, Gail Willenbring, Gaynor, Georgina Malisauskas, Gerrie, Gerry Buckel, Gert van Eck, Gertjan van Norel, Godfried Nijs, Graeme Whipps, Graham Russell, Grant Birley, Gregoire Deprez, Guillaume Laget, Hajare Ait Ouaba, Hans-Maarten, Harry Selwood, Hayley Young, Helen Ruiter, Hetty, Holly Matter, Howard Cheng, Ian Cooper, Ian Wiseman, Ineke, Ineke van Poelgeest, Ines Jonkers, Iona Baggerman, Ipek G. Kulahci, Isabel Kessler, Ivica Skokic, Jack Delves, Jacqueline Horkings, Jake Winters, Jamie McBean, Jan Twomet, Jane Herbert, Janeth Vargas, Jannie Bouwman, Jason Kurth, Jasper den Hollander, Javier Caldera Fernández de los Muros, Jaxon Hoffmann, Jayme, Jen

Browning, Jen Makin, Jen McDonald, Jendy Jalving, Jennifer, Jennifer Babin, Jennifer Bailey, Jennifer Docherty, Jennifer Falkofske, Jennifer Flor, Jennifer Giesbrecht, Jennifer Hendricks, Jennifer McIntosh, Jenny Atkinson, Jenny Clark, Jeremy Kuzub, Jeremy Mion, Jeremy Perez, Jerry Eklund, Jessica, Jessica Dorsey, Jessica Keller, Jessica Leanne, Jessica Pruter, Jessica Reurich, Jessica Taylor, Jill Silverberg, Joanna Fox, Joanne Kampinga, Jodan, Jodi Baker, Joe Cali, Joelka van Daal, John Oxley, Joke Foppen, Jonas Suni, Jose Luis Hormaechea, Jose Reynaga, Josefine Friedemann, Julia Sumerling, Julian Soldat, Julie Hayes, Julie Lawson, Jure Atanackov, Jørgen van Meijbeek, Kaetlyn, Kaitlyn Krus, Kaitlynn Williams, Kali Salmas, Karin Biermans, Kat Smith, Kate Cameron, Kate Draeger, Katharina Amon, Katherine, Kathy Janssen-Gubbels, Kathy Olson, Katie Giles, Katie Moloney, Katie Raymer-Woods, Kaveendra Daluwathumulla, Kayla, Kees Zwaan, Kellie Louise, Kelsey Harms, Ken, Kendall K., Kerri Johnson, Kevin, Kevin Kelleher, Kevin Palmer, Kezia Kurian, Khoi Nguyen, Kieran, Kim Hesse, Kimberly Shorkey, Kirsten Steele, Klaas Jobse, Kori Gill-Davidson, Kristina Young, Kylie Gee, Kyra Wing, Laura Hansen, Lauren Guenon, Laurie Crofoot, Lee K., Les Ladbrook, Leslie Mouncey, Liane Henry, Libby Gabriel, Lilian Kars, Lily Neyland, Linda, Linda S., Lindey, Lindsay Eastman, Lisa K. Hyatt, Lisa Starr, Liz Halliday, Liz Stuart, Loes Aartsen, Logan, Lone, Lotte Enting, Luc Jeanjean, Luke Rasmussen, Luke Verschoor, Lynn Sosnoskie, MJ van Hengel, Madalyn Draper, Malcolm Park, Mandy Erades, Manja, Manon Véber, Marcia Boomhouwer, Marco, Margaret Fitzgerald, Margaret Sonnemann, Margot Koorenhof, Marianne, Marianne Coppens, Marianne van den Berg, Marjan Spijkers, Marjon Wensink, Mark Egan, Mark N., Martha Loeppky, Martin van Marion, Martina, Martine, Martyn Lloyd, Marybeth Kiczenski, Maryla Machlick, Matthew Gaines, Matthew Pfab, Maxy, Meg, Megan Marsh, Melanie Clarke, Melanie Fama, Melissa, Melissa Kaelin, Merlijn, Mia Noyens, Michael Harmon, Michael Tomeh, Michelle, Michelle Bandy, Michelle Maynard, Michelle Stephenson, Mike Smith, Mirjam Jansen, Mirjam Leyte, Mirriam, Missy McCormick, Monique van Oijen, Monique, Montse, Morgan merrell, Nadia Tildesley, Nadja, Nanette Smith, Narelle, Natalie Pace, Natalie Sinkr, Natasha Peiskar, Nate Avish, Nepal Nelson Palma, Nicholas, Nicola Jackson, Nicolas Achmadi, Nicole Anderson, Nicole, Nicole P., Nicole Walton, Nicolás Concha Vargas, Nienke Huijsing, Nik Zimmermann, Nikita Loreggian, Nikki Boys, Nikki Dayton-Gelati, Niko, Niké Spits, Nory, Obbe, Oliver Saunders Wilder, Padmini Selvaganesan, Paige West, Pam & Andy Barnes, Pandora Biskner, Parmeet Singh, Pat Russell, Patricia, Patrick Johanneson, Paul Brooks, Paul West, Paul Williams, Paula Mair, Paulina, Pearl Wong, Peter Dohnt, Peter R. Grounds, Petra Bloemsma, Piet Berger, Pip Reisch, Pippa Mitchell, Poppy Franklin, Rachael Ramirez, Rachel Baxter, Randy Milanovic, Raul Saavedra, Raylene Garwood, Rebekah DeVinney, Remus, René Wolf, Ricardo Panuzzio, Ricardo Velasco, Richard Pyne, Ricki-Lee Teague, Rita Baker, Robbi James, Robert Fear, Robert-Jan, Robin Moon, Rolinde Hatzmann, Rona Hatzmann-Jorritsma, Roope Hakanpää, Rosie Cooper, Rosie Johnson, Ross Johnston, Rudy Siggs, Ryan Latterell, Ryan Voutilainen, Sabrina Spanjaart, Sandi, Sandra Alder, Sandra Stemmerik, Sankalp Merchant, Santosh Ramaswamy, Sarah H. Taft, Seamus FR, Serpollier Cléa, Shannon Landles, Shardae Ros, Sharon, Shaula Corr, Shawn Rosinski, Shawn Saito, Shellie Evans, Sherri Yezbick-Taylor, Shikhar Gupta, Shirley Jones, Sia Nikolaou, Silver Moon, Simon Evans, Sjon de Mol, Sonja Yearsley, Spencer Plovie, Stefan Ayto, Steve Brown, Steve DuBois, Sue Noble-Adams, Sunny Yang, Supriya, Susan Padfield, Susan Snow, Suze, Sylvia de Raat, Tammi Turner, Tammy Vallee, Tanya Melnik, Thomas Grandin, Théo Vischel, Tiffany Lamb, Titouan Joulain, Tom Warner, Tracey Parks, Traci Krzyzanowski, Tracie Blackburn, Travis Vander Laan, Tristan Pokornyi, Ursula Ram, Vaclav, Vanessa Wenners, Victoria Coleman, Vincent Ledvina, Vincent Morand, Virginia, Ward Van Herck, Wendy, Wendy Bakker-Coppens, Wendy Forsyth, Wendy Heugens, Wesley Souza, William McQuillan, Xavier Meneboode, Yolanda de Groot, Ytsje Kobus, Yvette Phillips, Yvo Ambags, Yvonne Heijboer, Zade Johnston, Zeel Parmar, Zia Self, and Zoe Alexander.

References

Akasofu, S.-I.: Long-standing unsolved problems in solar physics and magnetospheric physics, in: Multiscale Coupling of Sun-Earth Processes, edited by: Lui, A. T. Y., Kamide, Y., and Consolini, G., Elsevier Science B.V., Amsterdam, 71–82, ISBN 978-0-444-51881-1, https://doi.org/10.1016/B978-044451881-1/50006-X, 2005.

Alfonsi, L., Bergeot, N., Cilliers, P. J., De Franceschi, G., Baddeley, L., Correia, E., Di Mauro, D., Enell, C.-F., Engebretson, M., Ghoddousi-Fard, R., Häggström, I., Ham, Y.-b., Heygster, G., Jee, G., Kero, A., Kosch, M., Kwon, H.-J., Lee, C., Lotz, S., Macotela, L., Marcucci, M. F., Miloch, W. J., Morton, Y. J., Naoi, T., Negusini, M., Partamies, N., Petkov, B. H., Pottiaux, E., Prikryl, P., Shreedevi, P. R., Slapak, R., Spogli, L., Stephenson, J., Triana-Gómez, A. M., Troshichev, O. A., Van Malderen, R., Weygand, J. M., and Zou, S.: Review of Environmental Monitoring by Means of Radio Waves in the Polar Regions: From Atmosphere to Geospace, Surv. Geophys., 43, 1609–1698, https://doi.org/10.1007/s10712-022-09734-z, 2022.

Archer, W. E., St. -Maurice, J. P., Gallardo-Lacourt, B., Perry, G. W., Cully, C. M., Donovan, E., Gillies, D. M., Downie, R., Smith, J., and Eurich, D.: The Vertical Distribution of the Optical Emissions of a Steve and Picket Fence Event, Geophys. Res. Lett., 46, 10719–10725, https://doi.org/10.1029/2019GL084473, 2019.

Baker, D. N., Li, X., Pulkkinen, A., Ngwira, C. M., Mays, M. L., Galvin, A. B., and Simunac, K. D. C.: A major solar eruptive event in July 2012: Defining extreme space weather scenarios, Space Weather, 11, 585–591, https://doi.org/10.1002/swe.20097, 2013.

Bates, D. R.: The Intensity Distribution in the Nitrogen Band Systems Emitted from the Earth's Upper Atmosphere, P. Roy. Soc. Lond. Ser. A, 196, 217–250, https://doi.org/10.1098/rspa.1949.0025, 1949.

Bhatt, A. N., Harding, B. J., Makela, J. J., Navarro, L., Lamarche, L. J., Valentic, T., Kendall, E. A., and Venkatraman, P.: MANGO: An Optical Network to Study the Dynamics of the Earth's Upper Atmosphere, J. Geophys. Res.-Space, 128, e2023JA031589, https://doi.org/10.1029/2023JA031589, 2023.

Blake, S. P., Pulkkinen, A., Schuck, P. W., Glocer, A., and Tóth, G.: Estimating Maximum Extent of Auroral Equatorward Boundary Using Historical and Simulated Surface Magnetic Field Data, J. Geophys. Res.-Space, 126, e28284, https://doi.org/10.1029/2020JA028284, 2021.

Broadfoot, A. L.: Resonance scattering by N_2^+, Planet. Space Sci., 15, 1801–1815, https://doi.org/10.1016/0032-0633(67)90017-7, 1967.

Bruus, E.: Taivaanvahti/Himlakollen/Skywatcher's search interface, https://www.taivaanvahti.fi/app/docs/interface/output_interface_en.html, (last access: 19 December 2024), 2024.

Burrell, A., van der Meeren, C., and Laundal, K. M.: aburrell/aacgmv2: Version 2.6.0 [Software], Zenodo [code], https://doi.org/10.5281/zenodo.3598705, 2020.

Case, N. A., Kingman, D., and MacDonald, E. A.: A real-time hybrid aurora alert system: Combining citizen science reports with an auroral oval model, Earth Space Sci., 3, 257–265, https://doi.org/10.1002/2016EA000167, 2016a.

Case, N. A., MacDonald, E. A., and Viereck, R.: Using citizen science reports to define the equatorial extent of auroral visibility, Space Weather, 14, 198–209, https://doi.org/10.1002/2015SW001320, 2016b.

Donovan, E., Mende, S., Jackel, B., Frey, H., Syrjäsuo, M., Voronkov, I., Trondsen, T., Peticolas, L., Angelopoulos, V., Harris, S., Greffen, M., and Connors, M.: The THEMIS all-sky imaging array—system design and initial results from the prototype imager, J. Atmos. Sol.-Terr. Phys., 68, 1472–1487, https://doi.org/10.1016/j.jastp.2005.03.027, 2006.

Eastwood, J. P., Hapgood, M. A., Biffis, E., Benedetti, D., Bisi, M. M., Green, L., Bentley, R. D., and Burnett, C.: Quantifying the Economic Value of Space Weather Forecasting for Power Grids: An Exploratory Study, Space Weather, 16, 2052–2067, https://doi.org/10.1029/2018SW002003, 2018.

Enengl, F., Spogli, L., Kotova, D., Jin, Y., Oksavik, K., Partamies, N., and Miloch, W. J.: Investigation of Ionospheric Small-Scale Plasma Structures Associated With Particle Precipitation, Space Weather, 22, e2023SW003605, https://doi.org/10.1029/2023SW003605, 2024.

Evans, J. S., Correira, J., Lumpe, J. D., Eastes, R. W., Gan, Q., Laskar, F. I., Aryal, S., Wang, W., Burns, A. G., Beland, S., Cai, X., Codrescu, M., England, S., Greer, K., Krywonos, A., McClintock, W. E., Plummer, T., and Veibell, V.: GOLD Observations of the Thermospheric Response to the 10–12 May 2024 Gannon Superstorm, Geophys. Res. Lett., 51, e2024GL110506, https://doi.org/10.1029/2024GL110506, 2024.

Fang, X., Randall, C. E., Lummerzheim, D., Wang, W., Lu, G., Solomon, S. C., and Frahm, R. A.: Parameterization of monoenergetic electron impact ionization, Geophys. Res. Lett., 37, L22106, https://doi.org/10.1029/2010GL045406, 2010.

Foster, J. C., Erickson, P. J., Nishimura, Y., Zhang, S. R., Bush, D. C., Coster, A. J., Meade, P. E., and Franco-Diaz, E.: Imaging the May 2024 Extreme Aurora With Ionospheric Total Electron Content, Geophys. Res. Lett., 51, e2024GL111981, https://doi.org/10.1029/2024GL111981, 2024.

Gjerloev, J. W.: The SuperMAG data processing technique, J. Geophys. Res.-Space, 117, A09213, https://doi.org/10.1029/2012JA017683, 2012.

Grandin, M. and ARCTICS collaboration: Citizen Science Reports on Aurora Sighting and Technological Disruptions during the 10 May 2024 Geomagnetic Storm – ARCTICS Survey, Zenodo [data set], https://doi.org/10.5281/zenodo.12732615, 2024.

Grandin, M., Palmroth, M., Whipps, G., Kalliokoski, M., Ferrier, M., Paxton, L. J., Mlynczak, M. G., Hilska, J., Holmseth, K., Vinorum, K., and Whenman, B.: Large-Scale Dune Aurora Event Investigation Combining Citizen Scientists' Photographs and Spacecraft Observations, AGU Advances, 2, e00338, https://doi.org/10.1029/2020AV000338, 2021.

Green, J. L. and Boardsen, S.: Duration and extent of the great auroral storm of 1859, Adv. Space Res., 38, 130–135, https://doi.org/10.1016/j.asr.2005.08.054, 2006.

Greshko, M.: Extreme solar storm generated aurorae – and "surprise", Science Insider, 13 May 2024, https://doi.org/10.1126/science.zoakd5z, 2024.

Gritsevich, M., Lyytinen, E., Moilanen, J., Kohout, T., Dmitriev, V., Lupovka, V., Midtskogen, S., Kruglikov, N., Ischenko, A., Yakovlev, G., Grokhovsky, V., Haloda, J., Halodova, P., Peltoniemi, J., Aikkila, A., Taavitsainen, A., Lauanne, J., Pekkola,

M., Kokko, P., and Larionov, M.: First meteorite recovery based on observations by the Finnish Fireball Network, in: Proceedings of the International Meteor Conference, Giron, 162–169, France, ISBN 978-2-87355-028-8, 2014.

Hapgood, M., Angling, M. J., Attrill, G., Bisi, M., Cannon, P. S., Dyer, C., Eastwood, J. P., Elvidge, S., Gibbs, M., Harrison, R. A., Hord, C., Horne, R. B., Jackson, D. R., Jones, B., Machin, S., Mitchell, C. N., Preston, J., Rees, J., Rogers, N. C., Routledge, G., Ryden, K., Tanner, R., Thomson, A. W. P., Wild, J. A., and Willis, M.: Development of Space Weather Reasonable Worst Case Scenarios for the UK National Risk Assessment, Space Weather, 19, e2020SW002593, https://doi.org/10.1029/2020SW002593, 2021.

Hayakawa, H., Ebihara, Y., Mishev, A., Koldobskiy, S., Kusano, K., Bechet, S., Yashiro, S., Iwai, K., Shinbori, A., Mursula, K., Miyake, F., Shiota, D., Silveira, M. V. D., Stuart, R., Oliveira, D. M., Akiyama, S., Ohnishi, K., and Miyoshi, Y.: The Solar and Geomagnetic Storms in May 2024: A Flash Data Report, arXiv [preprint], https://doi.org/10.48550/arXiv.2407.07665, 2024.

He, F., Yao, Z., Ni, B., Cao, X., Ye, S., Guo, R., Li, J., Ren, Z., Yue, X., Zhang, Y., Wei, Y., Zhang, X., and Pu, Z.: Sawtooth and dune auroras simultaneously driven by waves around the plasmapause, Earth Planet. Phys., 7, 237–246, https://doi.org/10.26464/epp2023023, 2023.

Herlingshaw, K., Lach, D., Dayton-Oxland, R., Bruus, E., Karvinen, E., Ledvina, V., Partamies, N., Grandin, M., Spijkers, M., Nishimura, Y., Knudsen, D., Ladbrook, L., Martinis, C., Gallardo-Lacourt, B., Dyer, A., Mielke, L., Ratzlaff, C., Evans, L., Helin, M., Kuzub, J., Mathieu, B., Thomas, N., Glad, M., Donovan, E., Syrjäsuo, M., Cordon, S., Andersen, J., and Legg, C.: ARCTICS Aurora Field Guide And Handbook For Citizen Science, Zenodo, https://doi.org/10.5281/zenodo.13932081, 2024.

Johnsen, M. G.: Real-time determination and monitoring of the auroral electrojet boundaries, J. Space Weather Space Clim., 3, A28, https://doi.org/10.1051/swsc/2013050, 2013.

Karttunen, H.: Ursan historia: Tähtitieteellinen yhdistys Ursa 1921–2021, Tähtitieteellinen Yhdistys Ursa Ry, ISBN 9789525985986, 2021.

Kataoka, R., Miyoshi, Y., Shiokawa, K., Nishitani, N., Keika, K., Amano, T., and Seki, K.: Magnetic Storm-Time Red Aurora as Seen From Hokkaido, Japan on 1 December 2023 Associated With High-Density Solar Wind, Geophys. Res. Lett., 51, e2024GL108778, https://doi.org/10.1029/2024GL108778, 2024.

Kelso, T. S.: CelesTrak – Satellite Catalog (SATCAT) [data set], https://celestrak.org/satcat/search.php (last access: 19 December 2024), 2024.

Kosar, B. C., MacDonald, E. A., Case, N. A., and Heavner, M.: Aurorasaurus Database of Real-Time, Crowd-Sourced Aurora Data for Space Weather Research, Earth Space Sci., 5, 970–980, https://doi.org/10.1029/2018EA000454, 2018a.

Kosar, B. C., MacDonald, E. A., Case, N. A., Zhang, Y., Mitchell, E. J., and Viereck, R.: A case study comparing citizen science aurora data with global auroral boundaries derived from satellite imagery and empirical models, J. Atmos. Sol.-Terr. Phys., 177, 274–282, https://doi.org/10.1016/j.jastp.2018.05.006, 2018b.

Kwak, Y.-S., Kim, J.-H., Kim, S., Miyashita, Y., Yang, T., Park, S.-H., Lim, E.-K., Jung, J., Kam, H., Lee, J., Lee, H., Yoo, J.-H., Lee, H., Kwon, R.-Y., Seough, J., Nam, U.-W., Lee,

W. K., Hong, J., Sohn, J., Kwak, J., Kwak, H., Kim, R.-S., Kim, Y.-H., Cho, K.-S., Park, J., Lee, J., Nguyen, H. N. H., and Talha, M.: Observational Overview of the May 2024 G5-Level Geomagnetic Storm: From Solar Eruptions to Terrestrial Consequences, J. Astron. Space Sci., 41, 171–194, https://doi.org/10.5140/JASS.2024.41.3.171, 2024.

Ledvina, V., Brandt, L., MacDonald, E., Frissell, N., Anderson, J., Chen, T. Y., French, R. J., Di Mare, F., Grover, A., Battams, K., Sigsbee, K., Gallardo-Lacourt, B., Lach, D., Shaw, J. A., Hunnekuhl, M., Kosar, B., Barkhouse, W., Young, T., Kedhambadi, C., Ozturk, D. S., Claudepierre, S. G., Dong, C., Witteman, A., Kuzub, J., and Sinha, G.: Agile collaboration: Citizen science as a transdisciplinary approach to heliophysics, Front. Astron. Space Sci., 10, 1165254, https://doi.org/10.3389/fspas.2023.1165254, 2023.

Liang, J., Gillies, D. M., Spanswick, E., and Donovan, E. F.: Converting TREx-RGB green-channel data to 557.7 nm auroral intensity: Methodology and initial results, Earth Planet. Phys., 8, 258–274, https://doi.org/10.26464/epp2023063, 2024.

Lilensten, J. and Blelly, P. L.: The TEC and F2 parameters as tracers of the ionosphere and thermosphere, J. Atmos. Sol.-Terr. Phys., 64, 775–793, https://doi.org/10.1016/S1364-6826(02)00079-2, 2002.

Lu, G., Richmond, A. D., Lühr, H., and Paxton, L.: High-latitude energy input and its impact on the thermosphere, J. Geophys. Res.-Space, 121, 7108–7124, https://doi.org/10.1002/2015JA022294, 2016.

Lummerzheim, D. and Lilensten, J.: Electron transport and energy degradation in the ionosphere: Evaluation of the numerical solution, comparison with laboratory experiments and auroral observations, Ann. Geophys., 12, 1039–1051, https://doi.org/10.1007/s00585-994-1039-7, 1994.

MacDonald, E. A., Case, N. A., Clayton, J. H., Hall, M. K., Heavner, M., Lalone, N., Patel, K. G., and Tapia, A.: Aurorasaurus: A citizen science platform for viewing and reporting the aurora, Space Weather, 13, 548–559, https://doi.org/10.1002/2015SW001214, 2015.

MacDonald, E. A., Donovan, E., Nishimura, Y., Case, N. A., Gillies, D. M., Gallardo-Lacourt, B., Archer, W. E., Spanswick, E. L., Bourassa, N., Connors, M., Heavner, M., Jackel, B., Kosar, B., Knudsen, D. J., Ratzlaff, C., and Schofield, I.: New science in plain sight: Citizen scientists lead to the discovery of optical structure in the upper atmosphere, Sci. Adv., 4, eaaq0030, https://doi.org/10.1126/sciadv.aaq0030, 2018.

Malacara, D.: Color Vision and Colorimetry, Theory and Applications, SPIE Press, Bellingham, WA, USA, ISBN 0-8194-4228-3, 2011.

Martinis, C., Nishimura, Y., Wroten, J., Bhatt, A., Dyer, A., Baumgardner, J., and Gallardo-Lacourt, B.: First Simultaneous Observation of STEVE and SAR Arc Combining Data From Citizen Scientists, 630.0 nm All-Sky Images, and Satellites, Geophys. Res. Lett., 48, e2020GL092169, https://doi.org/10.1029/2020GL092169, 2021.

Martinis, C., Griffin, I., Gallardo-Lacourt, B., Wroten, J., Nishimura, Y., Baumgardner, J., and Knudsen, D. J.: Rainbow of the Night: First Direct Observation of a SAR Arc Evolving Into STEVE, Geophys. Res. Lett., 49, e98511, https://doi.org/10.1029/2022GL098511, 2022.

Mather, J.: Spectral and XYZ Color Functions, MATLAB Central File Exchange [code], https://www.mathworks.com/matlabcentral/fileexchange/7021-spectral-and-xyz-color-functions (last access: 19 December 2024), 2024.

Mende, S. B. and Turner, C.: Color Ratios of Subauroral (STEVE) Arcs, J. Geophys. Res.-Space, 124, 5945–5955, https://doi.org/10.1029/2019JA026851, 2019.

Moilanen, J. and Gritsevich, M.: Light scattering by airborne ice crystals – An inventory of atmospheric halos, J. Quant. Spectrosc. Ra., 290, 108313, https://doi.org/10.1016/j.jqsrt.2022.108313, 2022.

Newell, P. T. and Gjerloev, J. W.: Evaluation of SuperMAG auroral electrojet indices as indicators of substorms and auroral power, J. Geophys. Res.-Space, 116, A12211, https://doi.org/10.1029/2011JA016779, 2011.

Newell, P. T. and Gjerloev, J. W.: SuperMAG-based partial ring current indices, J. Geophys. Res.-Space, 117, A05215, https://doi.org/10.1029/2012JA017586, 2012.

Newell, P. T., Liou, K., Zhang, Y., Sotirelis, T., Paxton, L. J., and Mitchell, E. J.: OVATION Prime-2013: Extension of auroral precipitation model to higher disturbance levels, Space Weather, 12, 368–379, https://doi.org/10.1002/2014SW001056, 2014.

Nishimura, Y., Bruus, E., Karvinen, E., Martinis, C. R., Dyer, A., Kangas, L., Rikala, H. K., Donovan, E. F., Nishitani, N., and Ruohoniemi, J. M.: Interaction Between Proton Aurora and Stable Auroral Red Arcs Unveiled by Citizen Scientist Photographs, J. Geophys. Res.-Space, 127, e2022JA030570, https://doi.org/10.1029/2022JA030570, 2022.

Nishimura, Y., Dyer, A., Kangas, L., Donovan, E., and Angelopoulos, V.: Unsolved problems in Strong Thermal Emission Velocity Enhancement (STEVE) and the picket fence, Front. Astron. Space Sci., 10, 3, https://doi.org/10.3389/fspas.2023.1087974, 2023.

Nishitani, N., Ruohoniemi, J. M., Lester, M., Baker, J. B. H., Koustov, A. V., Shepherd, S. G., Chisham, G., Hori, T., Thomas, E. G., Makarevich, R. A., Marchaudon, A., Ponomarenko, P., Wild, J. A., Milan, S. E., Bristow, W. A., Devlin, J., Miller, E., Greenwald, R. A., Ogawa, T., and Kikuchi, T.: Review of the accomplishments of mid-latitude Super Dual Auroral Radar Network (SuperDARN) HF radars, Prog. Earth Planet. Sci., 6, 27, https://doi.org/10.1186/s40645-019-0270-5, 2019.

Oliveira, D. M., Zesta, E., Mehta, P. M., Licata, R. J., Pilinski, M. D., Tobiska, W. K., and Hayakawa, H.: The Current State and Future Directions of Modeling Thermosphere Density Enhancements During Extreme Magnetic Storms, Front. Astron. Space Sci., 8, 764144, https://doi.org/10.3389/fspas.2021.764144, 2021.

Oughton, E. J., Skelton, A., Horne, R. B., Thomson, A. W. P., and Gaunt, C. T.: Quantifying the daily economic impact of extreme space weather due to failure in electricity transmission infrastructure, Space Weather, 15, 65–83, https://doi.org/10.1002/2016SW001491, 2017.

Palmroth, M., Grandin, M., Helin, M., Koski, P., Oksanen, A., Glad, M. A., Valonen, R., Saari, K., Bruus, E., Norberg, J., Viljanen, A., Kauristie, K., and Verronen, P. T.: Citizen Scientists Discover a New Auroral Form: Dunes Provide Insight Into the Upper Atmosphere, AGU Adv., 1, e2019AV000133, https://doi.org/10.1029/2019AV000133, 2020.

Palmroth, M., Grandin, M., Sarris, T., Doornbos, E., Tourgaidis, S., Aikio, A., Buchert, S., Clilverd, M. A., Dandouras, I., Heelis, R., Hoffmann, A., Ivchenko, N., Kervalishvili, G., Knudsen, D. J., Kotova, A., Liu, H.-L., Malaspina, D. M., March, G., Marchaudon, A., Marghitu, O., Matsuo, T., Miloch, W. J., Moretto-Jørgensen, T., Mpaloukidis, D., Olsen, N., Papadakis, K., Pfaff, R., Pirnaris, P., Siemes, C., Stolle, C., Suni, J., van den IJssel, J., Verronen, P. T., Visser, P., and Yamauchi, M.: Lower-thermosphere–ionosphere (LTI) quantities: current status of measuring techniques and models, Ann. Geophys., 39, 189–237, https://doi.org/10.5194/angeo-39-189-2021, 2021.

Papitashvili, N. E. and King, J. H.: OMNI Hourly Data, NASA Space Physics Data Facility [data set], https://doi.org/10.48322/1shr-ht18, 2020.

Parker, W. E. and Linares, R.: Satellite Drag Analysis During the May 2024 Gannon Geomagnetic Storm, J. Spacecraft Rockets, 61, 1412–1416, https://doi.org/10.2514/1.A36164, 2024.

Picone, J. M., Hedin, A. E., Drob, D. P., and Aikin, A. C.: NRLMSISE-00 empirical model of the atmosphere: Statistical comparisons and scientific issues, J. Geophys. Res.-Space, 107, 1468, https://doi.org/10.1029/2002JA009430, 2002.

Robert, E., Barthelemy, M., Cessateur, G., Woelfflé, A., Lamy, H., Bouriat, S., Gullikstad Johnsen, M., Brändström, U., and Biree, L.: Reconstruction of electron precipitation spectra at the top of the upper atmosphere using 427.8 nm auroral images, J. Space Weather Space Clim., 13, 30, https://doi.org/10.1051/swsc/2023028, 2023.

Sandholt, P. E., Carlson, H. C., and Egeland, A.: Optical Aurora, Springer, Dordrecht, Netherlands, 33–51, ISBN 978-0-306-47969-4, https://doi.org/10.1007/0-306-47969-9_3, 2002.

Schnapf, J., Kraft, T., and Baylor, D.: Spectral sensitivity of human cone photoreceptors, Nature, 325, 439–441, https://doi.org/10.1038/325439a0, 1987.

Semeter, J., Hunnekuhl, M., MacDonald, E., Hirsch, M., Zeller, N., Chernenkoff, A., and Wang, J.: The Mysterious Green Streaks Below STEVE, AGU Adv., 1, e00183, https://doi.org/10.1029/2020AV000183, 2020.

Shepherd, S. G.: Altitude-adjusted corrected geomagnetic coordinates: Definition and functional approximations, J. Geophys. Res.-Space, 119, 7501–7521, https://doi.org/10.1002/2014JA020264, 2014.

Shiokawa, K., Otsuka, Y., and Connors, M.: Statistical Study of Auroral/Resonant-Scattering 427.8-nm Emission Observed at Subauroral Latitudes Over 14 Years, J. Geophys. Res.-Space, 124, 9293–9301, https://doi.org/10.1029/2019JA026704, 2019.

Sigernes, F., Dyrland, M., Brekke, P., Chernouss, S., Lorentzen, D. A., Oksavik, K., and Deehr, C. S.: Two methods to forecast auroral displays, J. Space Weather Space Clim., 1, A03, https://doi.org/10.1051/swsc/2011003, 2011.

Siscoe, G., Crooker, N. U., and Clauer, C. R.: Dst of the Carrington storm of 1859, Adv. Space Res., 38, 173–179, https://doi.org/10.1016/j.asr.2005.02.102, 2006.

Spogli, L., Alberti, T., Bagiacchi, P., Cafarella, L., Cesaroni, C., Cianchini, G., Coco, I., Di Mauro, D., Ghidoni, R., Giannattasio, F., Ippolito, A., Marcocci, C., Pezzopane, M., Pica, E., Pignalberi, A., Perrone, L., Romano, V., Sabbagh, D., Scotto, C., Spadoni, S., Tozzi, R., and Viola, M.: The effects of the May 2024 Mother's Day superstorm over the Mediterranean sector: from data to public communication, Ann. Geophys., 67, PA218, https://doi.org/10.4401/ag-9117, 2024.

Usoskin, I., Miyake, F., Baroni, M., Brehm, N., Dalla, S., Hayakawa, H., Hudson, H., Jull, A. J. T., Knipp, D., Koldobskiy, S., Maehara, H., Mekhaldi, F., Notsu, Y., Poluianov, S., Rozanov, E., Shapiro, A., Spiegl, T., Sukhodolov, T., Uusitalo, J., and Wacker, L.: Extreme Solar Events: Setting up a Paradigm, Space Sci. Rev., 219, 73, https://doi.org/10.1007/s11214-023-01018-1, 2023.

Whiter, D. K., Sundberg, H., Lanchester, B. S., Dreyer, J., Partamies, N., Ivchenko, N., Di Fraia, M. Z., Oliver, R., Serpell-Stevens, A., Shaw-Diaz, T., and Braunersreuther, T.: Fine-scale dynamics of fragmented aurora-like emissions, Ann. Geophys., 39, 975–989, https://doi.org/10.5194/angeo-39-975-2021, 2021.

Whiter, D. K., Partamies, N., Gustavsson, B., and Kauristie, K.: The altitude of green OI 557.7 nm and blue N_2^+ 427.8 nm aurora, Ann. Geophys., 41, 1–12, https://doi.org/10.5194/angeo-41-1-2023, 2023.